REPORT No.
CP/SEAM-2000/01

Structural Engineering and Applied Mechanics

Supplemental Viscous Damping Effects on Seismic Demands of Linear Elastic Systems

By
LINDA M. TAM and RAKESH K. GOEL

JUNE 15, 2000

DEPARTMENT OF CIVIL & ENVIRONMENTAL ENGINEERING
CALIFORNIA POLYTECHNIC STATE UNIVERSITY
SAN LUIS OBISPO, CA 93407

ABSTRACT

The objective of this study is to examine the effects of viscous supplemental damping on response quantities of asymmetric-plan structures responding in a linearly elastic fashion. The response quantities which will be investigated include: element deformations, base shears, and base torques. These response quantities will be normalized, evaluated, and then analyzed.

It is shown that supplemental damping is indeed effective in reducing element deformations and base torques. In some cases, supplemental damping is also effective in reducing base shears. In order to achieve the largest reduction in flexible element deformation, it is recommended that all fluid viscous dampers be placed on the flexible side. To produce the largest reduction in stiff element deformation, it is best to place all fluid viscous dampers on the stiff side.

Supplemental damping has a greater affect on total base shear than it does on total base torque. In some cases, it is recommended that a design for higher base shear forces be considered. Results from this investigation can be used to help in the design of such factors as foundation forces of structures.

ACKNOWLEDGMENTS

This research investigation is funded by the National Science Foundation under Grant No. CMS-9812414. This financial support is gratefully acknowledged. Linda M. Tam would also like to acknowledge CELSOC, Consulting Engineers and Land Surveyors of California, for providing financial support during last year of her study at Cal Poly.

This report is same, except for some editorial changes, as Linda M. Tam's master's thesis submitted to the California Polytechnic State University at San Luis Obispo. The thesis committee consisted of Professors Rakesh K. Goel (Chairman), Eric Kasper, and H. Mallareddy. The authors are thankful to Professors Kasper and Mallareddy for reviewing the thesis manuscript.

TABLE OF CONTENTS

LIST OF FIGURES

CHAPTER 1: INTRODUCTION

In order to achieve the best outcome to optimal performance of structures experiencing earthquake excitation, structures are required to "resist earthquakes through a combination of strength, deformability, and energy absorption [1]." Damping levels in structures, as well as the amount of energy dissipated during elastic behavior, are both very low. Structures remain intact during strong earthquakes because they have the ability to inelastically deform and go beyond the elastic limit. Inelastic deformation results in the increase of flexibility and energy dissipation, since it takes the form of localized plastic hinges. As a consequence, the structure can absorb a large portion of the earthquake energy through localized damage of the system, which also happens to resist lateral forces. By allowing the occurrence of some structural damage, effects of earthquakes can then be reduced.

Another way to reduce the dangerous effects of earthquakes can be to consider the distribution of energy within a structure. A certain amount of energy is input into a structure during an earthquake. This input energy is then changed into both kinetic and potential energy, which must either be absorbed or dissipated through heat. Vibrations would continue endlessly if there were no damping. However, since there is always some amount of inherent damping within the structure, energy is withdrawn from the system, and the amplitude of vibration is reduced until the motion stops. By adding some sort of supplemental damping device that will absorb a portion of the input energy from an earthquake, the structural performance of a building can be improved.

There are essentially two groups of systems which can improve the earthquake response performance: passive systems and active systems. Examples of passive systems include base isolation and supplemental mechanical damping. Active systems "require active participation of mechanical devices whose inputs depend upon measured building response [2]." Depending on the type of material used to transform energy to heat, damping devices can be split into four categories: viscous, friction, metallic yielding, and magnetic. Viscous material can be in the form of either liquid (silicone or oil) or solid (special rubbers or acrylics). Friction devices contain interface materials, such as steel to steel, copper with graphite to steel, or brake pad to steel. Metallic yielding devices most commonly use mild steel and lead. According to Hanson [2], the more "practical" devices for resisting earthquakes seem to be friction and metallic yielding devices.

The conservation of energy relationship can demonstrate how supplemental damping devices help improve structural performance by absorbing some of an earthquake's input energy:

$$E = E_k + E_s + E_h + E_d \qquad (1)$$

where E = the absolute energy input from the earthquake motion

E_k = the absolute kinetic energy

E_s = the recoverable elastic strain energy

E_h = the irrecoverable energy dissipated by the structural system through inelastic

or other forms of action

E_d = the energy dissipated by supplemental damping devices

The absolute energy input, E, contains the effect of inertia forces of the structure; it can also be thought of as the work done by the total base shear force at the foundation on the ground displacement.

By incorporating mechanical devices in the frame of the structure, energy is dissipated throughout the height of the structure. Energy dissipation can occur by any number of means: yielding of mild steel, sliding friction, motion of a piston within a viscous fluid, orificing of fluid, or viscoelastic action in rubber-like materials.

Many studies have supported the effectiveness of supplemental damping devices. However, most of these studies have concentrated on the seismic behavior of symmetric-plan systems; only recently has an effort begun towards examining the seismic response on asymmetric-plan systems.

Asymmetric-plan buildings have often been thought of as being undesirable because of their vulnerability to earthquakes due to coupled lateral and torsional motions. Some of the adverse effects of asymmetry include increased deformation, force, and ductility demands on lateral-load-resisting elements. The excessive deformations may lead to premature failure of brittle, non-ductile elements and may result in a sudden loss of the building's strength and stiffness leading to eventual failure. Excessive edge deformations may also cause pounding between closely spaced adjacent buildings and result in increased second-order (P-Δ) effects.

During the last couple of years, Goel [3] has engaged in researching the seismic behavior on asymmetric-plan systems with supplemental fluid viscous damping. Identified first were the main controlling parameters which characterized supplemental viscous damping and its plan-wise distribution. These parameters were noted to be: (1) the supplemental damping ratio, ζ_{sd} ; (2) the normalized supplemental damping eccentricity, $\bar{e}_{sd}$; and (3) the normalized supplemental damping radius of gyration, $\bar{\rho}_{sd}$. The amount of additional damping, as a fraction of the critical value, is indicated by ζ_{sd} , while the amount of uneven distribution of fluid viscous dampers located within the system plan is indicated by $\bar{e}_{sd}$. The amount of how much farther apart the center of supplemental damping (CSD) is from the fluid viscous dampers is indicated by $\bar{\rho}_{sd}$. The normalized supplemental damping radius of gyration, $\bar{\rho}_{sd}$, also indicates damping in the torsional mode of vibration of the corresponding symmetric-plan system.

After the identification of these three parameters, the effects of supplemental damping on asymmetric-plan systems were examined. When comparing the distribution of supplemental dampers in asymmetric-plan systems as opposed to symmetric plan-systems, it was found that an asymmetric distribution led to higher reductions in edge deformations. The results also showed that supplemental damping reduces edge deformations for both the flexible edge as well as the stiff edge. The degree of reduction, however, depends heavily on the normalized supplemental damping eccentricity, $\bar{e}_{sd}$. In order to achieve the largest reduction for the flexible edge, $\bar{e}_{sd}$ should take on the largest

negative value; while, for the stiff edge, the largest reduction occurs for the largest positive value of $\bar{e}_{sd}$. These findings suggest that the center of supplemental damping should be placed on the opposite side of the center of rigidity if the largest reduction for the flexible edge is desired. Otherwise, if the largest reduction for the stiff edge is desired, then the center of supplemental damping should be placed on the same side as the center of rigidity. It is important to note that the flexible edge is normally considered the most critical edge in asymmetric-plan systems because of the higher deformations induced by earthquakes.

Although the studies done by Goel [3] have led to significant improvement in the understanding of how plan-wise distribution of supplemental damping influences the deformations, it will also be useful to investigate the effects on foundation forces, such as base shear and base torque. Therefore, the objective of this investigation is to examine the effects of supplemental viscous damping on base shears and base torques. For completeness, a brief discussion on deformations is also included.

Chapter 2 presents a review on the different types of energy-absorbing devices and the way they function. Included in this discussion are: friction devices, metallic devices, viscoelastic dampers, and fluid viscous dampers. There is a brief section on other design considerations at the end of this chapter.

Chapter 3 discusses the method of investigation. A description and figure of the one-story model are given and an overview of the two ground motions that were used is also described. Included are figures of time-history plots and response spectra. A brief overview of which system parameters were selected is also given.

An analysis of the results is presented in chapter 4. Examined in this chapter are investigations on how plan-wise distribution of supplemental damping influences such quantities as: element deformations, base shears, and base torques. The damping devices studied are fluid viscous dampers. Figures of the normalized quantities are included as visual aids.

The conclusion is presented in chapter 5. An evaluation of the results is summarized here, as well as the importance of how this research can be used later in design.

CHAPTER 2: ENERGY ABSORBING SYSTEMS

2.1 Friction Devices

Figure 1 shows the design of a friction device proposed by Pall [6,7]. When seismic load is applied, the compression brace buckles as the tension brace induces slippage at the friction joint. As this happens, four links are activated, which then force the compression brace to slip. In this way, energy is dissipated in both braces while they are designed to be effective in tension only.

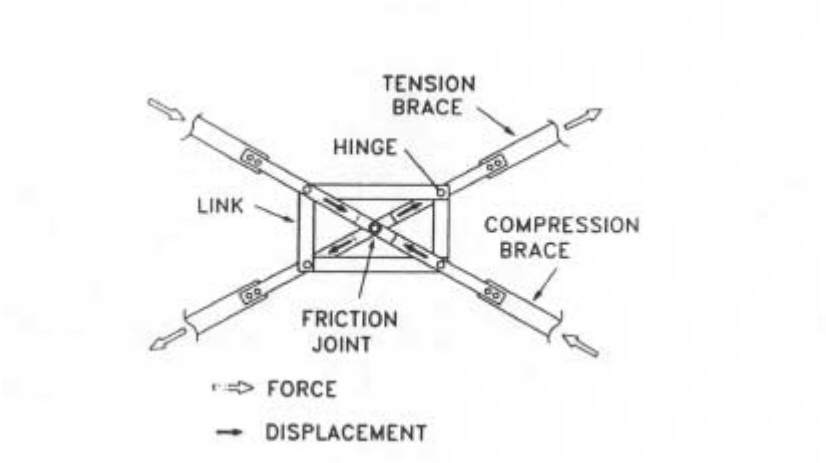

Figure 1. Friction damping device [6]

Filiatrault [8] and Aiken [9] conducted experimental studies on friction devices. They showed that friction devices could enhance structural performance by providing an increase in energy dissipation capacity, while reducing drifts when compared to moment-resisting frames. The reductions in story shear forces, however, were only moderate.

Figure 2 illustrates the construction of a Sumitomo [10] friction damper, which was developed by Sumitomo Metal Industries of Japan. For a number of years, the Sumitomo friction damper was manufactured for railway applications, but is now being extended to structural engineering. This device is made up of copper pads impregnated with graphite in contact with steel casing. Development of load on the contact surface is brought about by a series of wedges acting under compression of washer springs. The graphite's purpose is to lubricate the contact, so that silent operation is ensured.

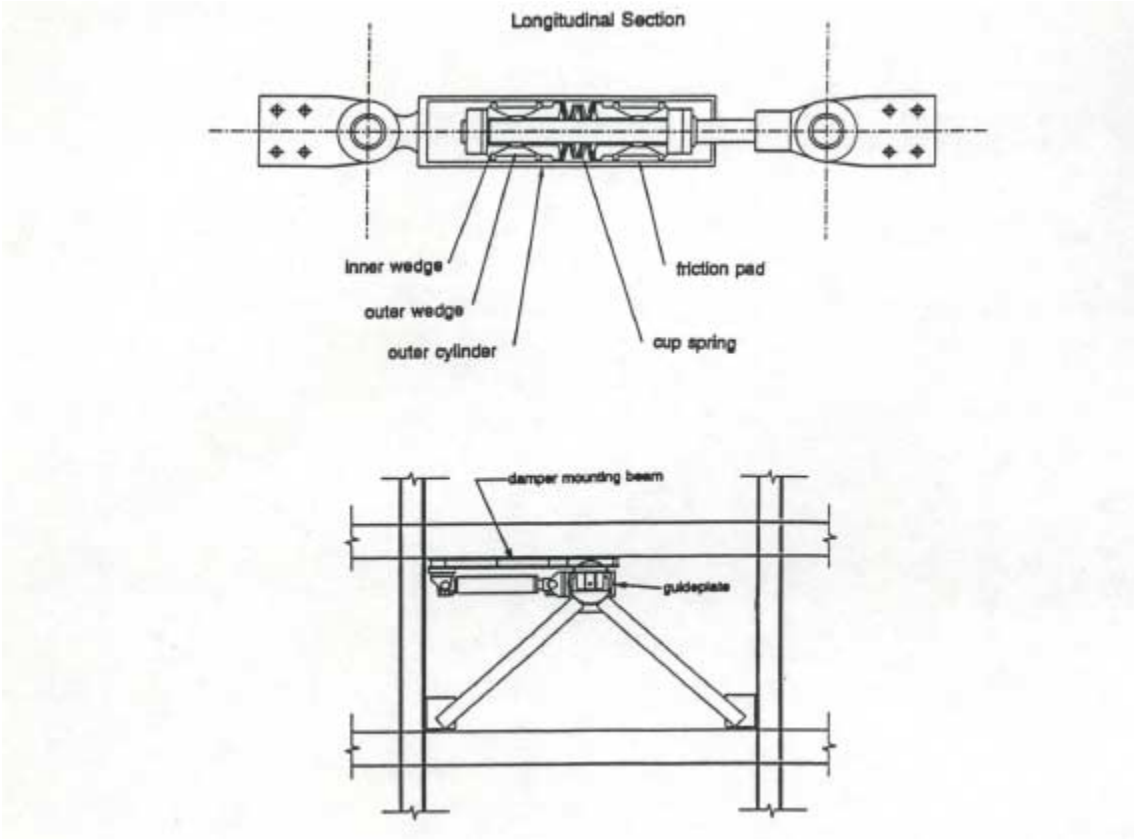

Figure 2. Sumitomo friction damper and installation detail [10]

Aiken [10] conducted experimental studies on Sumitomo dampers. The dampers were installed in a 9-story model structure and tested on a shake table. Instead of being installed diagonally as braces, the dampers were placed parallel to the floor beams. One of their ends was attached to a floor beam above, while the other end was attached to a chevron brace arrangement, which was attached to the floor beam below. The chevron braces were designed to be very stiff, while a special arrangement was used at the connection of each damper to the chevron brace to prevent lateral loading of the device.

Experimental studies on the performance of Sumitomo dampers resulted in conclusions that were similar to those on the study of Pall's friction bracing devices. In general, Aiken found that displacements were reduced when compared to moment-resisting frames, but that the amount of reduction was dependent on the input motion. He also found that the recorded base shear forces were of the same order as those of the moment-resisting frame. For optimum performance, it was found that the friction force at each level should be carefully selected based on the results of nonlinear dynamic analyses.

2.2 Metallic Devices

Many mild steel devices have been developed in New Zealand [11,12]. Some of these devices have been tested at U.C. Berkeley as parts of seismic isolation systems [23], and others have been widely used in seismic isolation applications in Japan [24]. Figure 3 shows details of a yielding steel bracing system which was installed in a

building in New Zealand. An important characteristic of the element is that the compression brace disconnects from the rectangular steel frame so that buckling is prevented and pinched hysteretic behavior does not occur [13]. Dissipation of energy occurs by inelastic deformation of the rectangular steel frame in the diagonal direction of the tension brace.

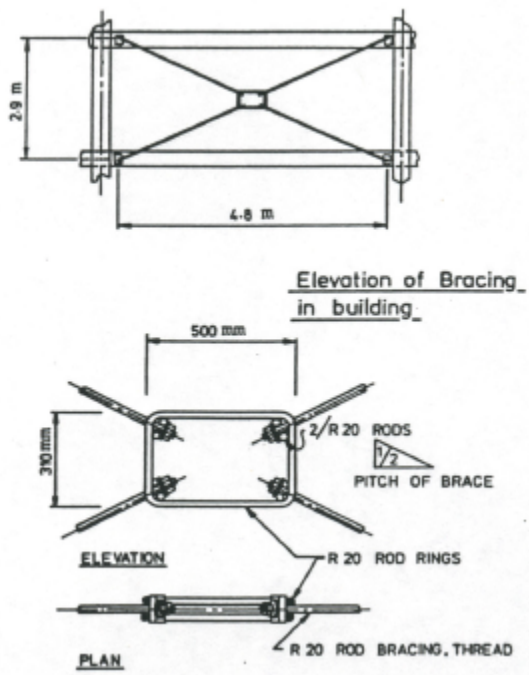

Figure 3. Details of a yielding steel bracing system [13]

Another element, which has been studied by Whittaker [14], is called the 'added damping and stiffness' (ADAS) device. The ADAS device shown in Figure 4 consists of multiple x-steel plates. The shape of the device is such that yielding occurs over the entire length, while the use of rigid boundary members ensure that the x-plates are deformed in double curvature.

Whittaker [14] performed shake table tests of a 3-story steel model structure. He demonstrated that ADAS elements improved the behavior of moment-resisting frames by increasing its stiffness, strength, and ability to dissipate energy. ADAS elements yield in a manner that is pre-determined, and they relieve excessive ductility demands from the moment frame. Just recently, ADAS elements have been used in the seismic retrofitting of the Wells Fargo Bank, a 2-story concrete building in San Francisco.

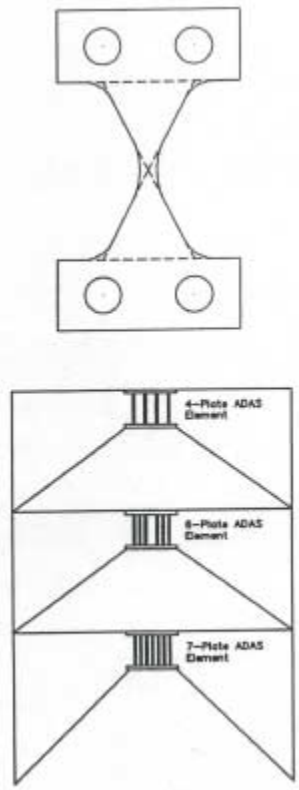

Figure 4. ADAS x-shaped steel plate and installation detail [14]

2.3 Viscoelastic Dampers

Viscoelastic dampers are made of bonded viscoelastic layers (acrylic polymers), in which the behavior of the viscoelastic dampers is controlled by the behavior in shear of the viscoelastic layers. They have been developed by the 3M Company and used in the control of wind vibration applications. Examples of where these dampers have been used include: the 110-story World Trade Center in New York, the 73-story Columbia Sea First Building in Seattle, and the 60-story Number Two Union Square Building in Seattle. Lin [15], Aiken [10], and Chang [16] have all conducted experimental studies on the performance of viscoelastic dampers, which can be seen in figure 5.

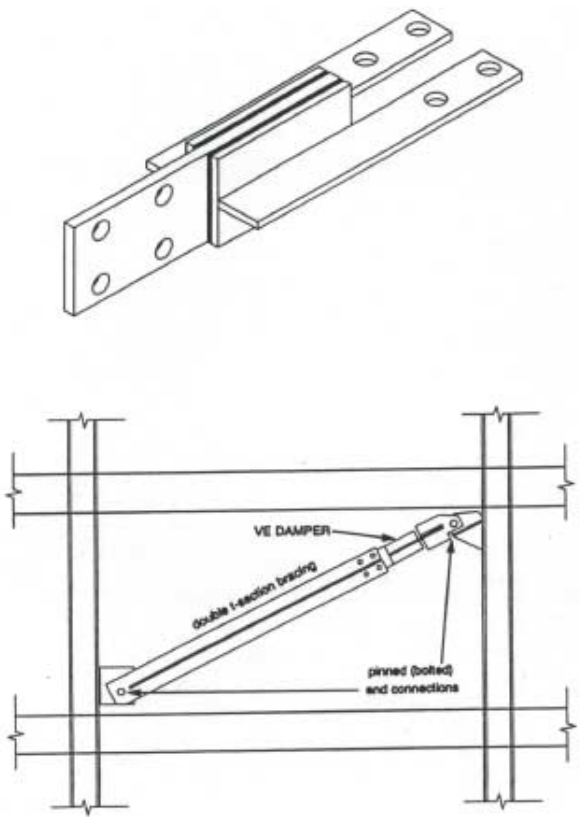

Figure 5. Viscoelastic damper and installation detail [10]

The shake table tests of Lin [15], Aiken [10], and Chang [16] demonstrated that the use of viscoelastic dampers contributed to significant benefits. Aiken's [10] tests showed that the addition of viscoelastic dampers led to interstorey drift reductions when compared to those of the moment-resisting frame. The ratio of interstorey drift in the viscoelastically damped structure to the interstorey drift in the moment-resisting frame was around 0.5 to 0.9. Base shear forces in the viscoelastically damped structure were about the same as those in the moment-resisting frame.

One major concern which needs to be accounted for during the design stage is the temperature dependency of viscoelastic dampers. A potential problem may arise in a symmetric viscoelastically damped structure in which either the dampers on one face of the structure or the dampers in the upper floors are at a higher temperature. This effect will cause the viscoelastically damped structure to exhibit either asymmetry in plan or vertical irregularity.

During testing, several delamination failures of viscoelastic dampers were reported by Aiken [10]. These delamination failures were attributed to the development of tensile stresses. He recommended that viscoelastic dampers be fitted with a bolt directly through the damper, which would help to prevent spreading of the steel plates.

2.4 Fluid Viscous Dampers

Fluid viscous dampers operate on the principle of fluid flow through orifices. They were originated in the late 1950's for the use in steel mills as energy absorbing buffers on overhead cranes. Variations of these devices were used as canal lock buffers and offshore oil rig leg suspensions. They were extensively utilized for the shock

isolation systems of aerospace and military hardware. Figure 6 illustrates the construction of this device. The fluid viscous damper is filled with silicone oil, and it consists of a stainless steel piston with a bronze orifice head and an accumulator. A passive bi-metallic thermostat allows the operation of this device over a temperature range of -40°F to 160°F. The fluid damper generates a force due to a difference in pressure across the piston head. This force in the fluid damper may be expressed as:

$$P = bp_{12} \qquad (2)$$

where p_{12} is the pressure differential in chambers 1 and 2, and b is a constant [1]. The constant b is a function of the piston head area, piston rod area, orifice area, number of orifices, control valve area, and the orifice and control valve discharge coefficients.

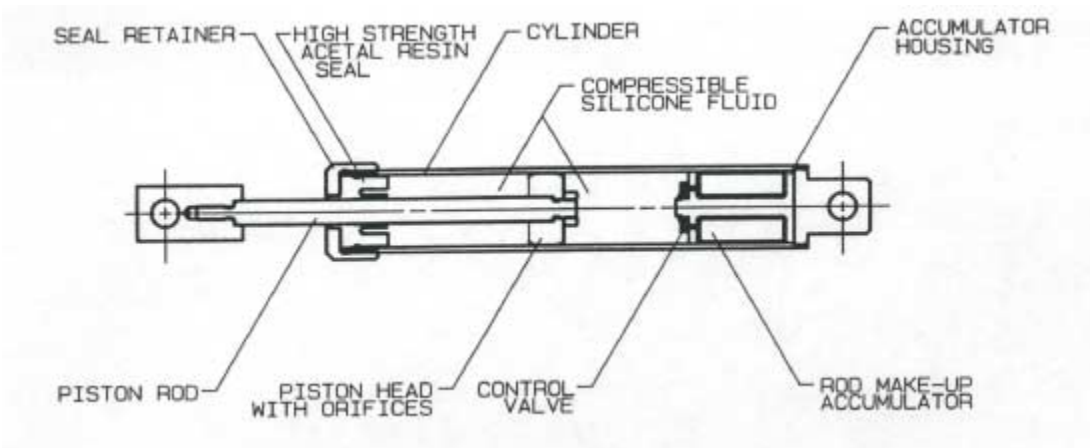

Figure 6. Construction of fluid viscous damper [17]

Experimental studies on fluid viscous dampers have shown that storey drifts can be reduced by 30% to 70%. Also, when comparing fluid dampers to viscoelastic, friction, and yielding steel dampers, it has been shown that fluid dampers outperform all other energy dissipating systems in the reduction of storey shear forces by 40% to 70%. The cause for this difference is attributed to the fluid damper's nearly pure linear viscous behavior.

2.5 Other Design Considerations

Aside from the addition of supplemental damping devices, which may be used during the seismic retrofit of a structure, it may also be necessary to strengthen the columns. Since drift is not the only concern in design, consideration must also be given to the significant amount of axial column forces, which may be induced depending on the force-displacement characteristics of the energy-absorbing devices. Significant axial column forces may lead to column compression failure, especially when the additional axial force happens to be in-phase with the peak drift.

A study by Goel [25] has examined the influence of inclined viscous dampers on column axial forces in a simple one-story frame building for harmonic loading and earthquake ground motion. It is noted that harmonic loading enables the development of a closed-form solution for the column axial force, while a closed-form solution for the peak values of the axial forces is not possible for earthquake loading. Values for the earthquake loading are, therefore, obtained by tracking the time history of axial forces.

Systems with horizontal dampers, i.e., $\theta = 0°$, have maximum axial forces which are due only to an elastic component. The maximum axial force in a system with horizontal dampers is perfectly in-phase with the elastic forces [25]. Systems with inclined dampers, however, have maximum axial forces which are due to both elastic as well as damping components. The maximum axial force in a system with inclined dampers has a phase lag and is not perfectly in-phase with the elastic forces.

The ratio of the peak force in a system with an inclined damper to the peak force in a system with a horizontal damper is used as an indicator of the amplification of the column axial force due to the inclined damper. Results show that the column axial force can be significantly higher in a system with an inclined damper than the column axial force in a system with a horizontal damper, even when the damping ratio in both systems is the same. The axial force amplification becomes larger as the frequency ratio increases, which indicates that the amplification of column axial forces will be large in either systems with low natural vibration frequency or systems subjected to excitations containing very high frequency contents. The amplification factor also increases as the value of the damping ratio increases.

Results also show that the phase lag between the column axial force and the elastic component can be significant. The phase lag increases with increasing values of frequency ratio and damping ratio. Peak values of column axial forces occur somewhere in between the peak elastic force and the peak damping force.

For earthquake ground motion, the N-S component of the ground acceleration recorded during the 1940 El Centro earthquake is selected. Results indicate that for very-short period systems less than 0.25 seconds, the axial force amplification is small. For longer period systems, however, the amplification becomes much more significant. The largest amplification tends to occur for systems with a period of around 0.8 seconds. It is again noted that the amplification increases with increasing values of damping ratio.

Similar trends are expected to apply to other ground motions, but the peak amplification may occur at a different period value. So far, the results computed for the selected earthquake ground motion support the findings based on simple harmonic loading. Future studies extended for multistory buildings will be very useful.

CHAPTER 3: METHODOLOGY

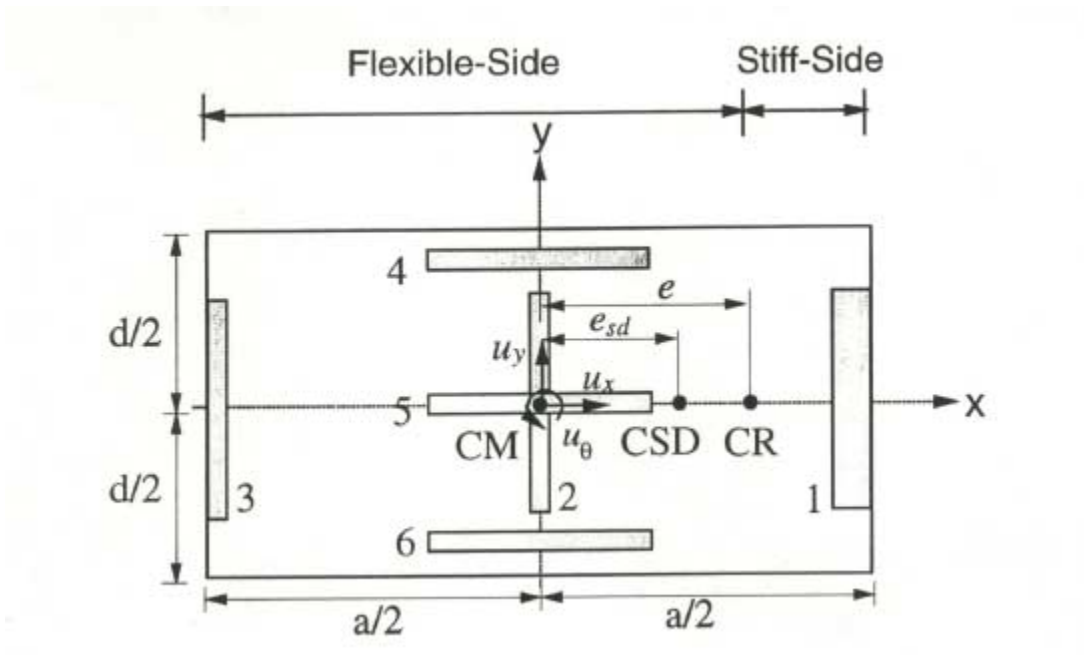

Figure 7. Idealized one-story system [3]

3.1 Model of One-Story System

The one-story system used previously by Goel [3] has been adapted for this investigation and can be seen in figure 7. This system consists of a rigid deck supported by six structural elements, (walls, columns, moment-frames, braced-frames, etc.) which are placed in two orthogonal directions. Incorporated into the bracing system are fluid viscous dampers. Assumptions are made that the mass properties of the system are symmetric about both the x- and y- axis, while the stiffness and damper properties are symmetric only about the x-axis.

The center of mass (CM) of the system is defined as the centroid of inertia forces when the system is subjected to a uniform translational acceleration in the direction under consideration. The CM coincides with the geometric center of the deck since the mass is uniformly distributed about both the x- and y-axis.

The center of supplemental damping (CSD) is defined as the centroid of damper forces when the system is subjected to a uniform translational velocity in the direction under consideration. The lack of symmetry in the damper properties about the y-axis is characterized by the supplemental damping eccentricity, e_{sd} , defined as the distance between the CM and the CSD.

The center of rigidity (CR) is defined as the point on the deck through which application of a static horizontal force causes no rotation of the deck [20]. For the one-story system considered here, the CR is also the centroid of resisting forces in structural elements when the system is subjected to a uniform translational displacement in the direction under consideration. The lack of symmetry in the stiffness properties about the y-axis is characterized by the stiffness eccentricities, e , defined as the distance between

the CM and the CR. With both CM and CR defined, the element that is on the same side of the CM as the CR is denoted as the stiff element, while the other element is designated as the flexible element.

3.2 Ground Motions

The first ground motion that is considered is the North-South component recorded at El Centro during the 1940 Imperial Valley earthquake. The peak values of ground acceleration, velocity, and displacement recorded at this site are 312.7 cm/s^2, 33.12 cm/s, and 21.34 cm, respectively. The acceleration time history of this ground motion is presented in figure 8, while the corresponding 5% - damped linear response spectrum is presented in figure 9.

The second ground motion that is considered is the 90° component recorded at the Sylmar County Hospital during the 1994 Northridge earthquake. The peak values of ground acceleration, velocity, and displacement recorded at this site are 592.6 cm/s^2, 76.94 cm/s, and 15.22 cm, respectively. The acceleration time history of this ground motion is presented in figure 10, while the corresponding 5% - damped linear response spectrum is presented in figure 11.

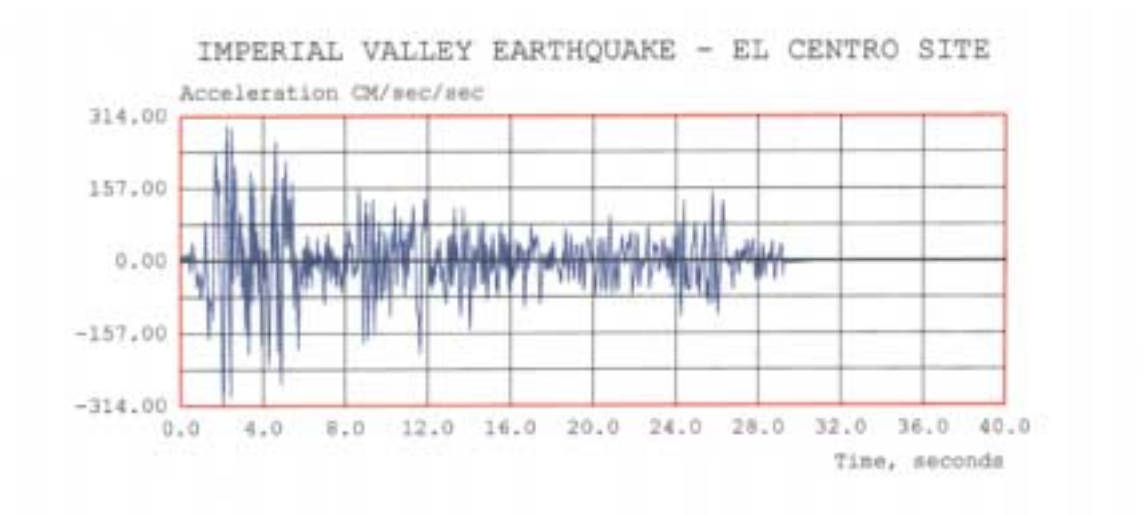

Figure 8. Time-history response of North-South component of ground acceleration recorded at El Centro during the Imperial Valley earthquake on May 18, 1940 (Using NONLIN)

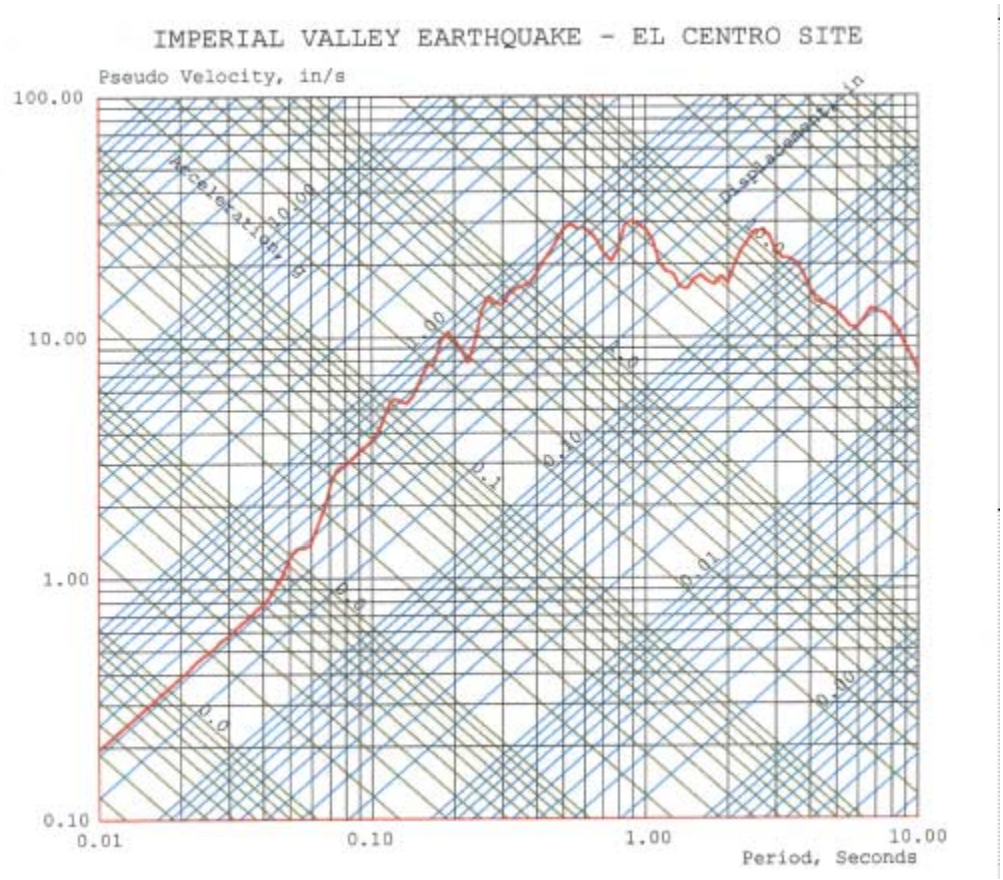

Figure 9. Response spectrum for North-South component of the ground motion recorded at El Centro during the Imperial Valley earthquake; ζ=5% (Using NONLIN)

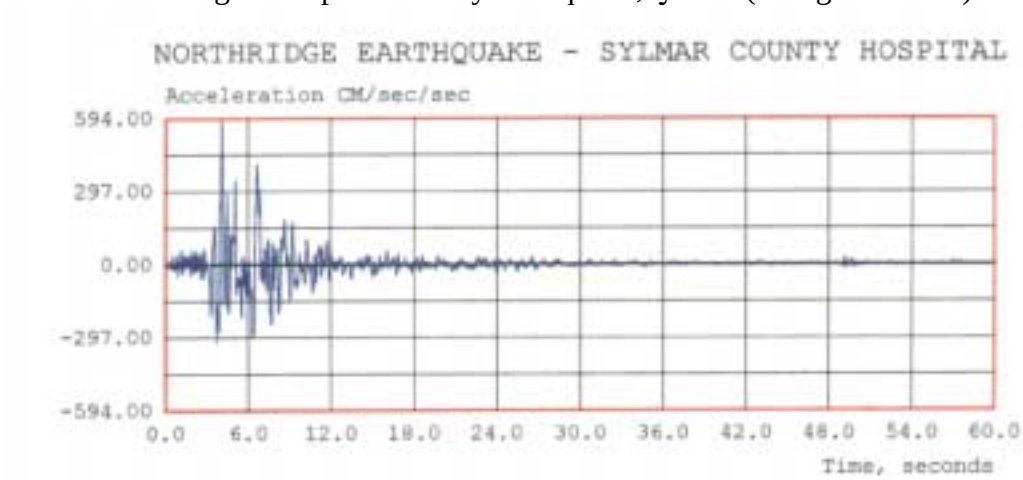

Figure 10. Time-history response of 90° component of ground acceleration recorded at Sylmar County Hospital during the 1994 Northridge earthquake (Using NONLIN)

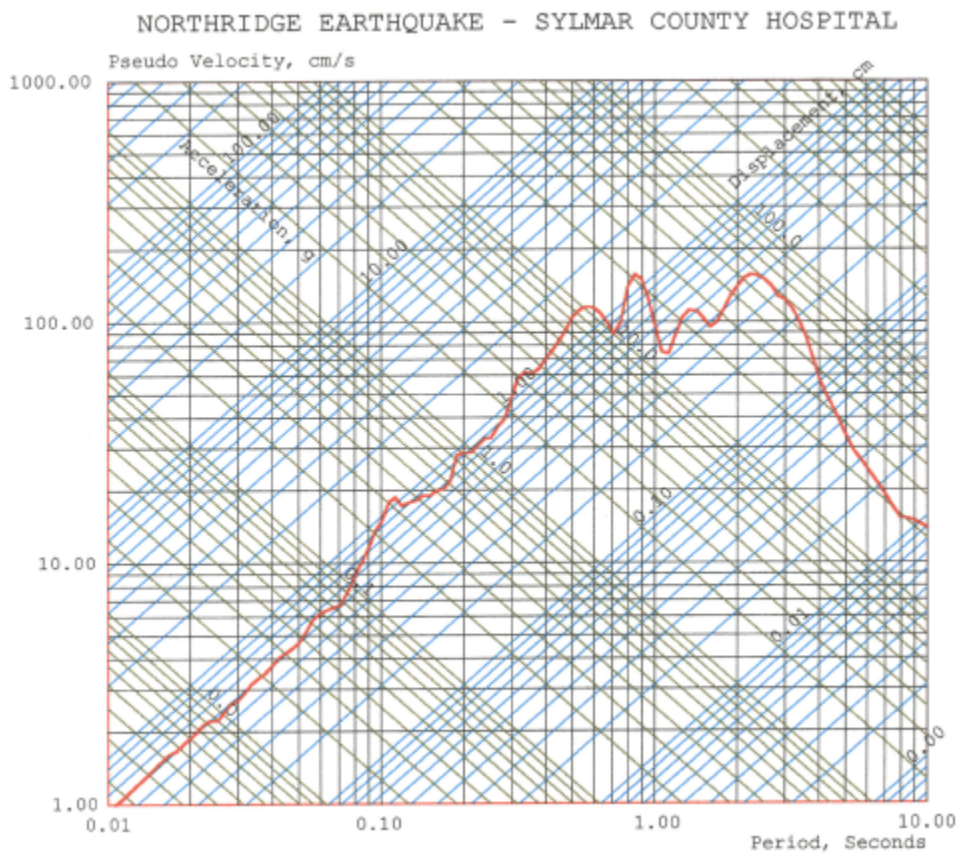

Figure 11. Response spectrum for 90° component of the ground motion recorded at the Sylmar County Hospital during the 1994 Northridge earthquake; ζ=5% (Using NONLIN)

3.3 Selection of System Parameters

Linear elastic analysis was performed for earthquake excitation only in the y-direction. In order to represent many low-rise and mid-rise buildings, values of T_y were selected to range from 0.05 seconds to 3 seconds. The ratio of the torsional frequency to transverse frequency, Ω_θ, was selected to be 1, so that systems with strong coupling between lateral and torsional motions in the elastic range would be represented. The ratio of x-direction to y-direction vibration frequencies, Ω_x, was also selected to equal 1. The aspect ratio, α, was chosen to be 2, while the damping ratio, ζ, remained fixed at 5%. Values for the stiffness eccentricities in the x-direction and y-direction were selected to be $\bar{e}_x = 0.2$ and $\bar{e}_y = 0$. Detailed descriptions of parameters that control elastic seismic response of asymmetric-plan buildings without supplemental damping were reported elsewhere [3]. The supplemental damping ratio, ζ_{sd}, remained fixed at 10%, while the normalized supplemental damping radius of gyration, $\bar{\rho}_{sd}$, was chosen to be 0.2 to represent a medium spread of the supplemental damping about the CSD. The three values of normalized supplemental damping eccentricities, $\bar{e}_{sd}$, were chosen to be: 0.2, 0, and -0.2. The first value, $\bar{e}_{sd} = 0.2$, corresponds to the coincidental location of the center of rigidity to the CSD. The second value, $\bar{e}_{sd} = 0$, corresponds to the identical location of the center of mass to the CSD. The third value, $\bar{e}_{sd} = -0.2$, corresponds to

the location of the CSD being on the opposite side of the center of mass from the center of rigidity.

CHAPTER 4: RESULTS

4.1 Effects of Supplemental Damping on Element Deformation

The first investigation examines how normalized element deformations of different normalized supplemental damping eccentricities ($\bar{e}_{sd} = e_{sd} \div a$, where a is the plan dimension of the system along the x-axis) vary with the transverse vibration period, T_y . The response quantities selected for this research are the deformations of the flexible and stiff elements in asymmetric system with supplemental damping normalized by the deformations of the flexible and stiff elements in asymmetric system without supplemental damping, $\bar{u}_f = u_{f,sd} \div u_f$ and $\bar{u}_s = u_{s,sd} \div u_s$. If the value of the normalized element deformation is more than one, this indicates that there are larger element deformations with supplemental damping than without supplemental damping. Likewise, if the value of the normalized element deformation is less than one, the opposite is true, i.e., there are smaller element deformations with supplemental damping than without supplemental damping.

Figure 12 presents normalized deformations for the flexible element, $\bar{u}_f$, due to the 1940 El Centro earthquake. As can be seen from this figure, all values for $\bar{u}_f$ are less than one. This is an indication that supplemental damping is effective in reducing flexible element deformations. The largest reduction of displacement is produced when using a supplemental damping eccentricity of –0.2, whereas the smallest reduction is produced when using a supplemental damping eccentricity of 0.2. These results lead to the recommendation of placing all fluid viscous dampers on the flexible side in order to obtain the largest reduction. This kind of placement suggests that the CSD should be on the opposite side of the center of rigidity.

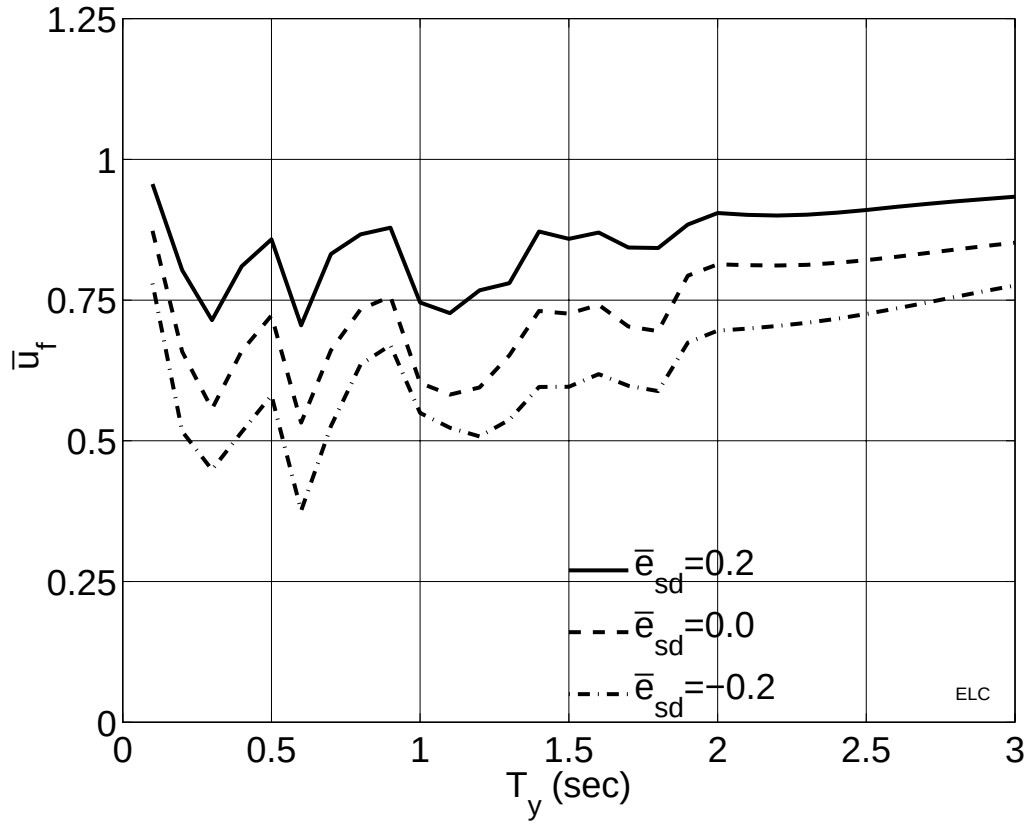

Figure 12. Normalized element deformations in asymmetric-plan systems of flexible side due to El Centro earthquake ($\bar{e}_x$=0.2; $\bar{e}_y$=0; Ω_θ=1; Ω_x=1; α=2; ζ=5%) with supplemental damping (ζ_{sd}=10%; $\bar{\rho}_{sd}$=0.2)

Figure 13 presents normalized deformations for the stiff element, $\bar{u}_s$, due to the 1940 El Centro earthquake. Observing from this figure, values for $\bar{u}_s$ are mostly close to or less than one. This leads to the indication that supplemental damping is effective in reducing element deformations on the stiff side. The largest reduction of displacement is produced by using a supplemental eccentricity of 0.2, while the smallest reduction is produced by using $\bar{e}_{sd}$ = -0.2. These results suggest that it would be best to place all fluid viscous dampers on the stiff side, such that the CSD will be on the same side as the center of rigidity.

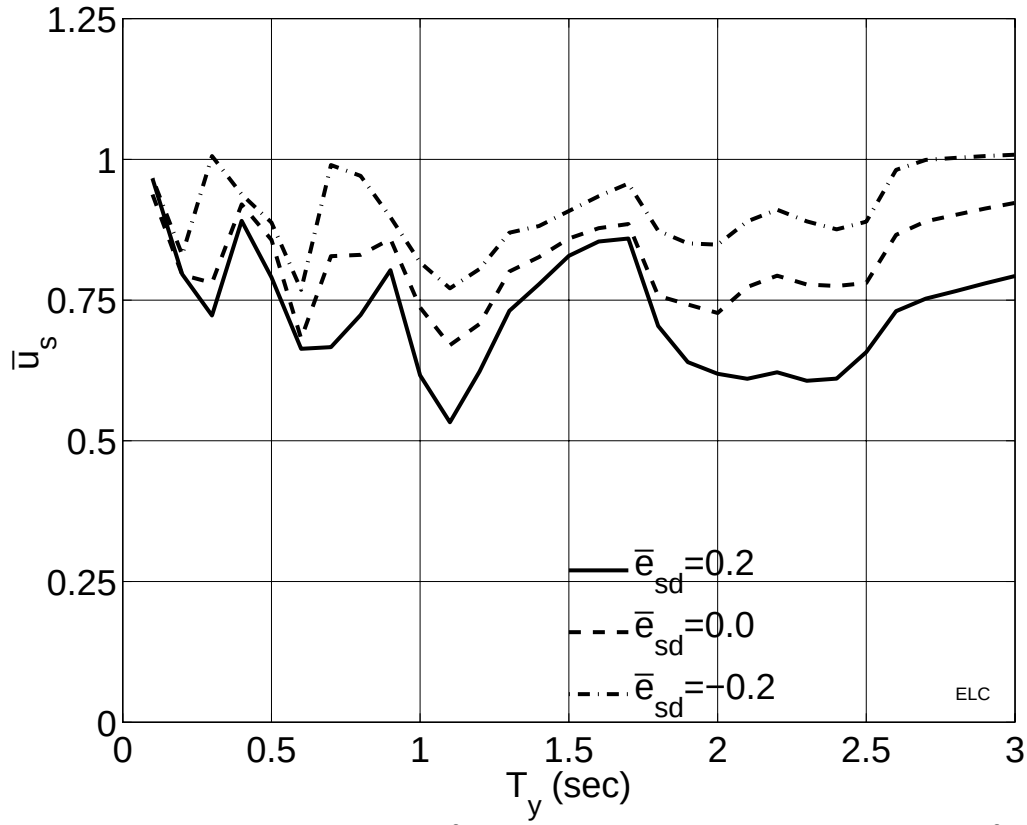

Figure 13. Normalized element deformations in asymmetric-plan systems of stiff side due to El Centro earthquake ($\bar{e}_x$=0.2; $\bar{e}_y$=0; Ω_θ=1; Ω_x=1; α=2; ζ=5%) with supplemental damping (ζ_{sd}=10%; $\bar{\rho}_{sd}$=0.2)

In order to examine how the trends observed for the 1940 El Centro earthquake will hold for a near source earthquake, results were next generated for the ground motion recorded at the Sylmar County Hospital parking lot during the 1994 Northridge earthquake. The results are shown in Figures 14 and 15. Figure 14 shows that all values for $\bar{u}_f$ are less than one. Supplemental damping indeed helps to decrease element deformations on the flexible side. By using a supplemental damping eccentricity of –0.2, the largest reduction of displacement can be achieved. The smallest reduction is achieved when the supplemental damping eccentricity is equal to 0.2. By placing all fluid viscous dampers on the flexible side, the flexible element deformation can be reduced the most. This means that the CSD will be on the opposite side of the center of rigidity.

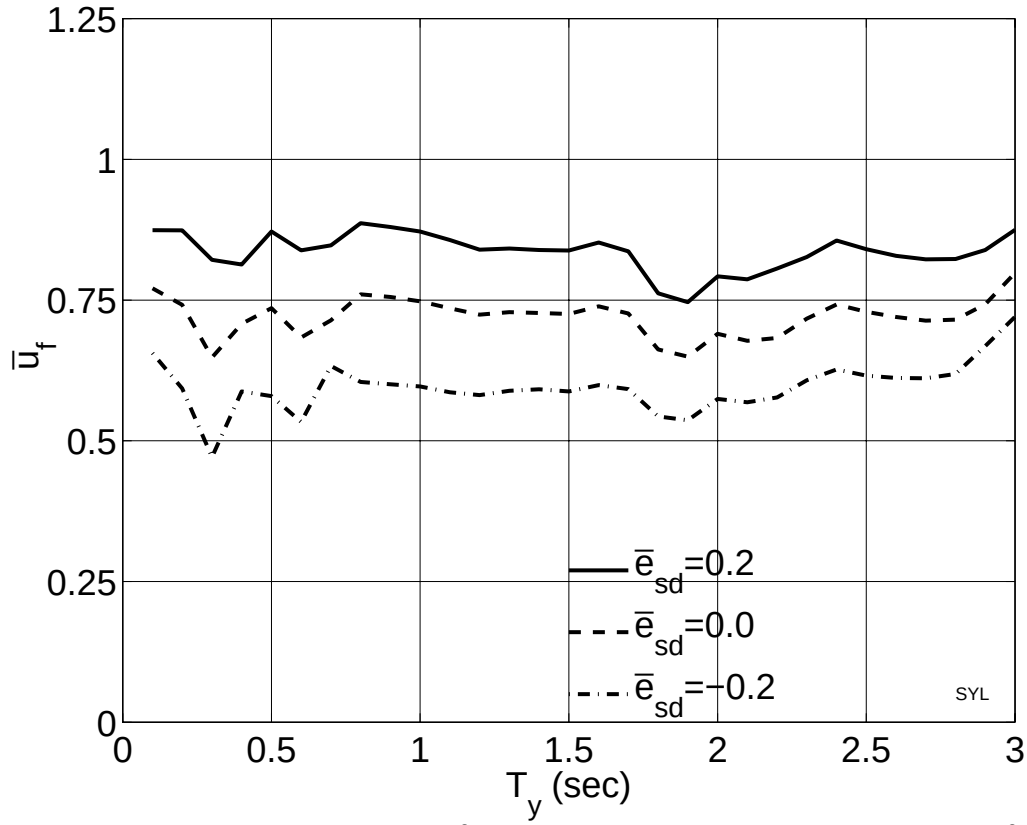

Figure 14. Normalized element deformations in asymmetric-plan systems of flexible side due to Sylmar earthquake ($\bar{e}_x$=0.2; $\bar{e}_y$=0; Ω_θ=1; Ω_x=1; α=2; ζ=5%) with supplemental damping (ζ_{sd}=10%; $\bar{\rho}_{sd}$=0.2)

Figure 15 shows the results of normalized deformations for the stiff element, $\bar{u}_s$, due to the Sylmar earthquake. For periods between 0.38 seconds and 0.60 seconds, values for $\bar{e}_{sd}$ = -0.2 are greater than one. All other values, however, are less than one and indicate that supplemental damping helps to reduce element deformations on the stiff side. For periods greater than 0.60 seconds, the largest reduction of displacement can be obtained by using $\bar{e}_{sd}$ = 0.2, while the smallest reduction can be obtained by using $\bar{e}_{sd}$ = -0.2. It is recommended that all fluid viscous dampers be placed on the stiff side in order to achieve the largest reduction of element deformation. The CSD, therefore, will remain on the same side as the center of rigidity.

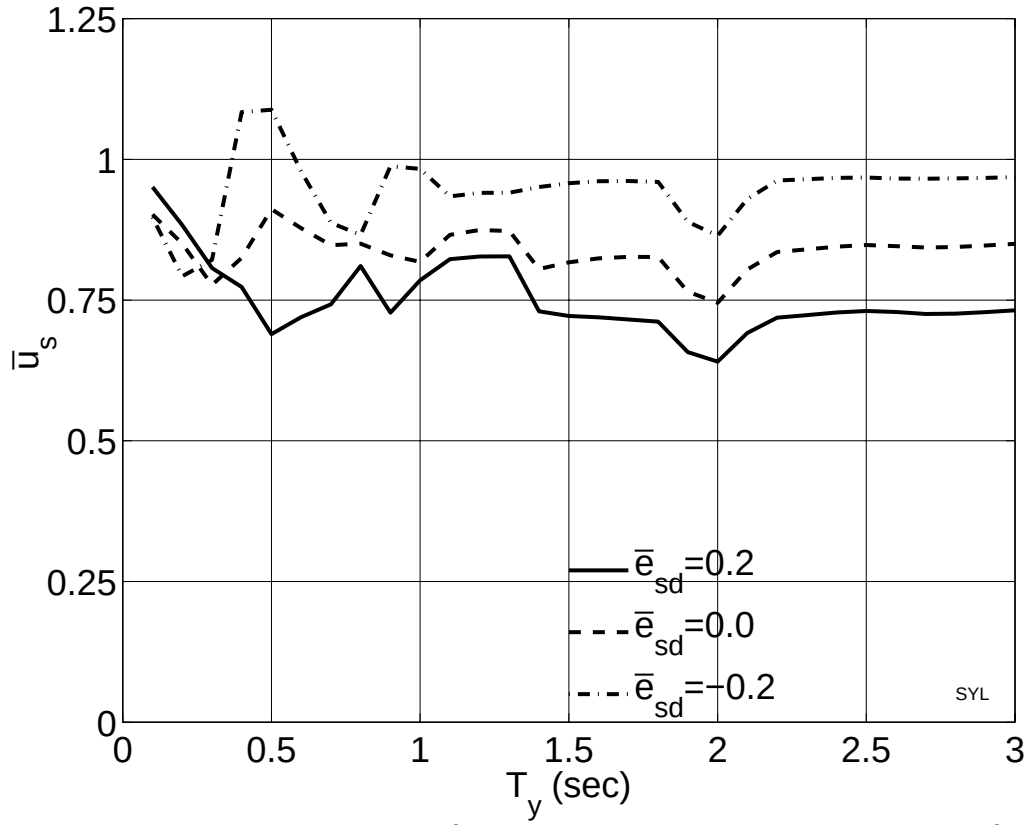

Figure 15. Normalized element deformations in asymmetric-plan systems of stiff side due to Sylmar earthquake ($\bar{e}_x$=0.2; $\bar{e}_y$=0; Ω_θ=1; Ω_x=1; α=2; ζ=5%) with supplemental damping (ζ_{sd}=10%; $\bar{\rho}_{sd}$=0.2)

The results presented so far indicate that the trends observed for the near-field ground motion are similar to those obtained for a broad-band earthquake like the El Centro.

4.2 Effects of Supplemental Damping on Base Shear

The second investigation examines how plan-wise distribution of supplemental damping influences normalized base shears. The response quantity selected is the base shear in asymmetric-plan system with supplemental damping normalized by the base shear in asymmetric-plan system without supplemental damping, $\bar{V}_b = V_{b,sd} \div V_b$. For a better understanding of which forces govern the total base shear, the total normalized base shear is broken down into further components, mainly the base shear due to elastic forces and the base shear due to damping forces.

Figure 16 shows the results of total normalized base shears, due to the El Centro earthquake. For $\bar{e}_{sd}$ = 0.2, most values of $\bar{V}_b$ are less than one. Exceptions where $\bar{V}_b$ is greater than one for $\bar{e}_{sd}$ = 0.2 occur for periods between 1.7 seconds and 1.85 seconds, as well as for periods between 2.8 seconds and 2.9 seconds. Within these regions where $\bar{V}_b$ is greater than one, base shears with supplemental damping are higher than base

shears without supplemental damping. For $\bar{e}_{sd}$ = 0, most values of $\bar{V}_b$ are also less than one. Values where $\bar{V}_b$ is less than one indicate that base shears with supplemental damping are less than base shears without supplemental damping. Exceptions where $\bar{V}_b$ is greater than one for $\bar{e}_{sd}$ = 0 occur for periods between 1.6 seconds and 1.9 seconds, as well as for periods between 2.6 seconds and 3.0 seconds. For $\bar{e}_{sd}$ = -0.2, values where $\bar{V}_b$ are greater than one occur for periods between 0.7 seconds and 0.9 seconds, as well as for periods between 1.5 seconds and 3.0 seconds. For $\bar{e}_{sd}$ = -0.2, values of $\bar{V}_b$ for all other periods are less than one. The trend of base shear seems to increase as the period increases.

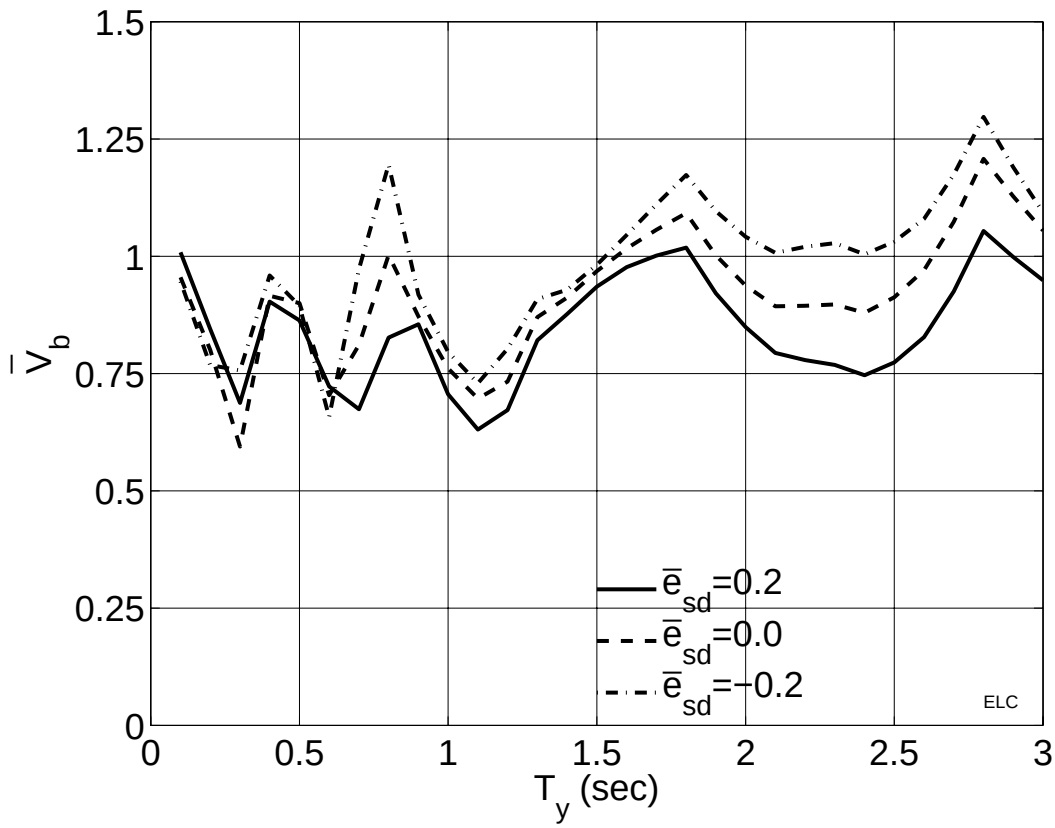

Figure 16. Normalized total base shears in asymmetric-plan systems due to El Centro earthquake ($\bar{e}_x$=0.2; $\bar{e}_y$=0; Ω_θ=1; Ω_x=1; α=2; ζ=5%) with supplemental damping (ζ_{sd}=10%; $\bar{\rho}_{sd}$=0.2)

In order to examine how much contribution of the total base shear is due to elastic forces and how much is due to damping forces, figures 17 and 18 show the results of both elastic base shears and damping base shears. Both elastic base shears and damping base shears are computed when the total base shear is at a maximum. Figure 17 shows that the trend of the elastic component of the normalized base shear seems to decrease as the period increases. Figure 18 shows the opposite trend, i.e., the damping component of the normalized base shear increases as the period increases. It can be seen from these figures that the damping forces and elastic forces are not necessarily 90° out of phase, and that the addition of damping forces contributes to higher total base shears.

This occurs because earthquake loading is transient in nature and conclusions based on harmonic loading may not necessarily be applicable to this type of loading.

Note that elastic forces and damping forces are 90° out of phase only during steady-state response of a single-degree-of-freedom system due to a single harmonic loading. If both elastic forces and damping forces reach a maximum value at the same time, then it can be said that both of these forces are in-phase. If one of these forces reaches a maximum while the other force is equal to zero, then it can be said that the elastic force and damping force are 90° out of phase; this 90° phase lag holds true for steady-state vibration.

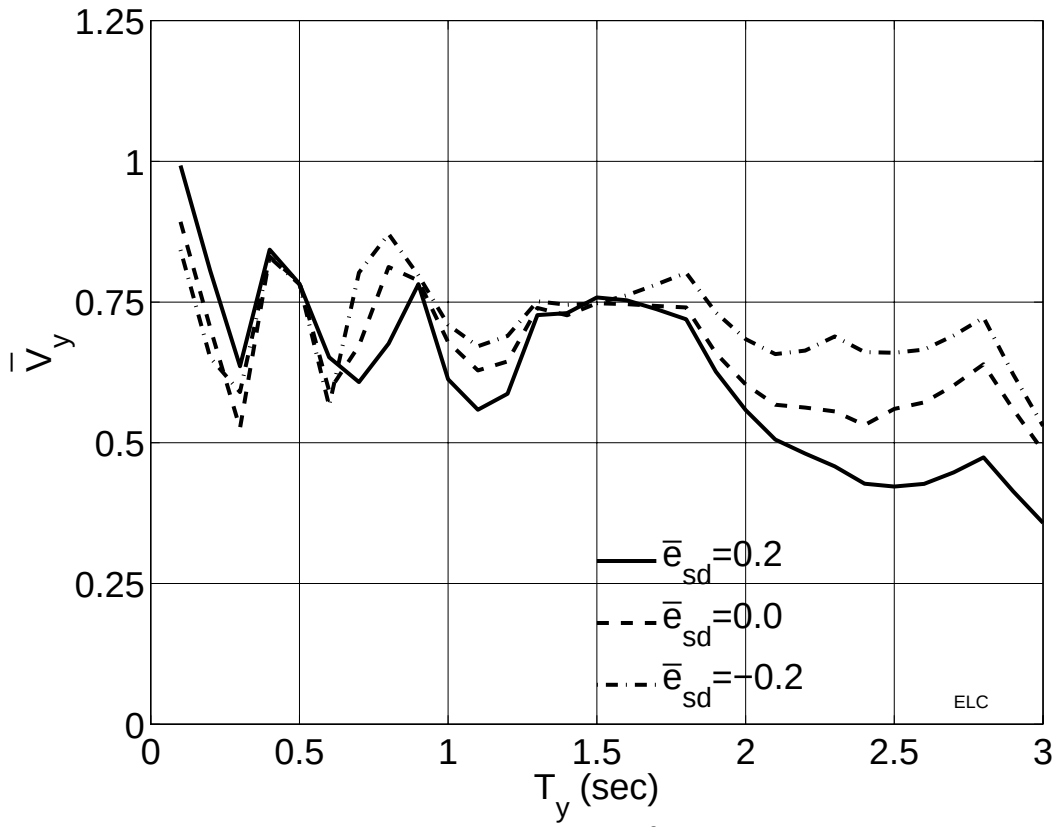

Figure 17. Normalized base shears due to elastic forces computed when total base shear is at a maximum in asymmetric-plan systems due to El Centro earthquake ($\bar{e}_x$=0.2; $\bar{e}_y$=0; Ω_θ=1; Ω_x=1; α=2; ζ=5%) with supplemental damping (ζ_{sd}=10%; $\bar{\rho}_{sd}$=0.2)

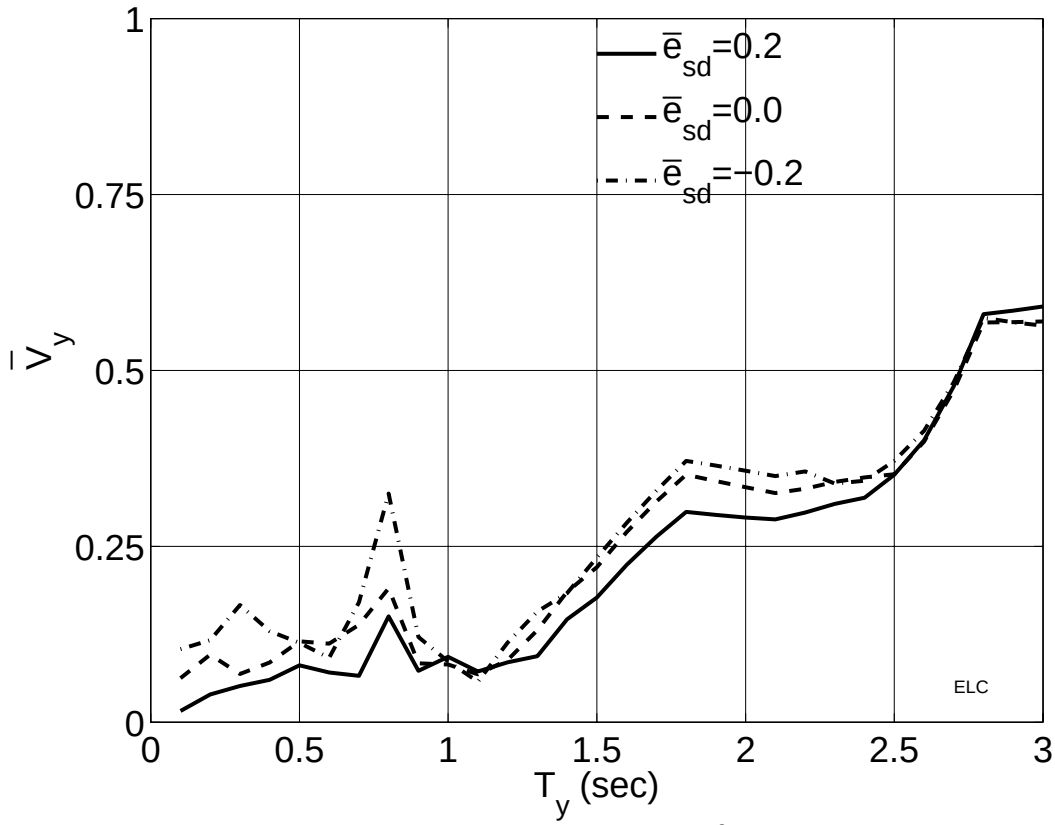

Figure 18. Normalized base shears due to damping forces computed when total base shear is at a maximum in asymmetric-plan systems due to El Centro earthquake ($\bar{e}_x$=0.2; $\bar{e}_y$=0; Ω_θ=1; Ω_x=1; α=2; ζ=5%) with supplemental damping (ζ_{sd}=10%; $\bar{\rho}_{sd}$=0.2).

Next, to see whether or not the trends observed for the 1940 El Centro earthquake will hold for a near source earthquake, results were generated for the ground motion recorded at the Sylmar County Hospital during the 1994 Northridge earthquake. Figure 19 shows the results of total normalized base shears, due to the Sylmar earthquake. For both $\bar{e}_{sd}$ = 0.2 and $\bar{e}_{sd}$ = 0, all values of $\bar{V}_b$ are less than one. When values of $\bar{V}_b$ are less than one, this implies that supplemental damping is effective in reducing base shears. For $\bar{e}_{sd}$ = -0.2, values where $\bar{V}_b$ are greater than one occur for periods between 0.5 seconds and 0.7 seconds, as well as for periods between 1.25 seconds and 1.75 seconds, and also for periods between 2.7 seconds and 3.0 seconds. For $\bar{e}_{sd}$ = -0.2, values of $\bar{V}_b$ for all other periods are less than one. Within regions where $\bar{V}_b$ is greater than one, base shears with supplemental damping are higher than base shears without supplemental damping. The largest reduction of base shear can be achieved by using $\bar{e}_{sd}$ = 0.2. However, when it is not possible to design with $\bar{e}_{sd}$ = 0.2, it is suggested that a design for higher base shear forces be considered.

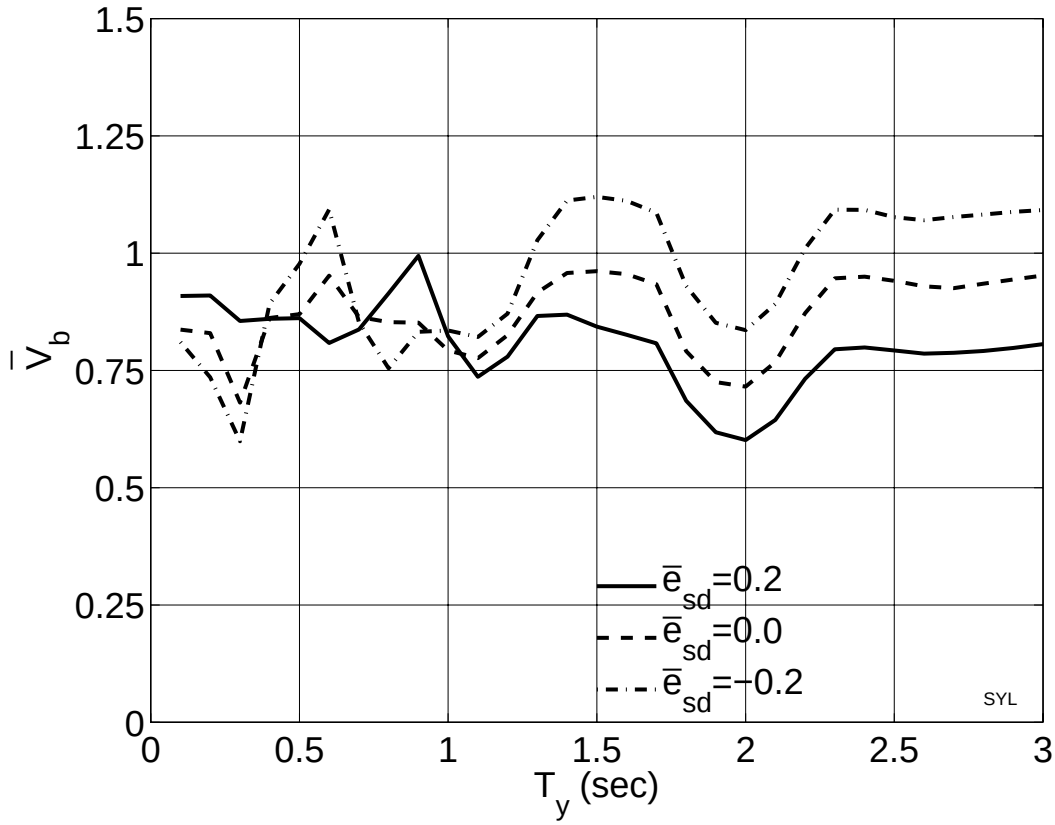

Figure 19. Normalized total base shears in asymmetric-plan systems due to Sylmar earthquake ($\bar{e}_x$=0.2; $\bar{e}_y$=0; Ω_θ=1; Ω_x=1; α=2; ζ=5%) with supplemental damping (ζ_{sd}=10%; $\bar{\rho}_{sd}$=0.2)

Due to the Sylmar earthquake, figures 20 and 21 depict the contributions of the total base shear due to elastic forces and damping forces. Both the elastic base shears and damping base shears are computed when the total base shear is at a maximum.

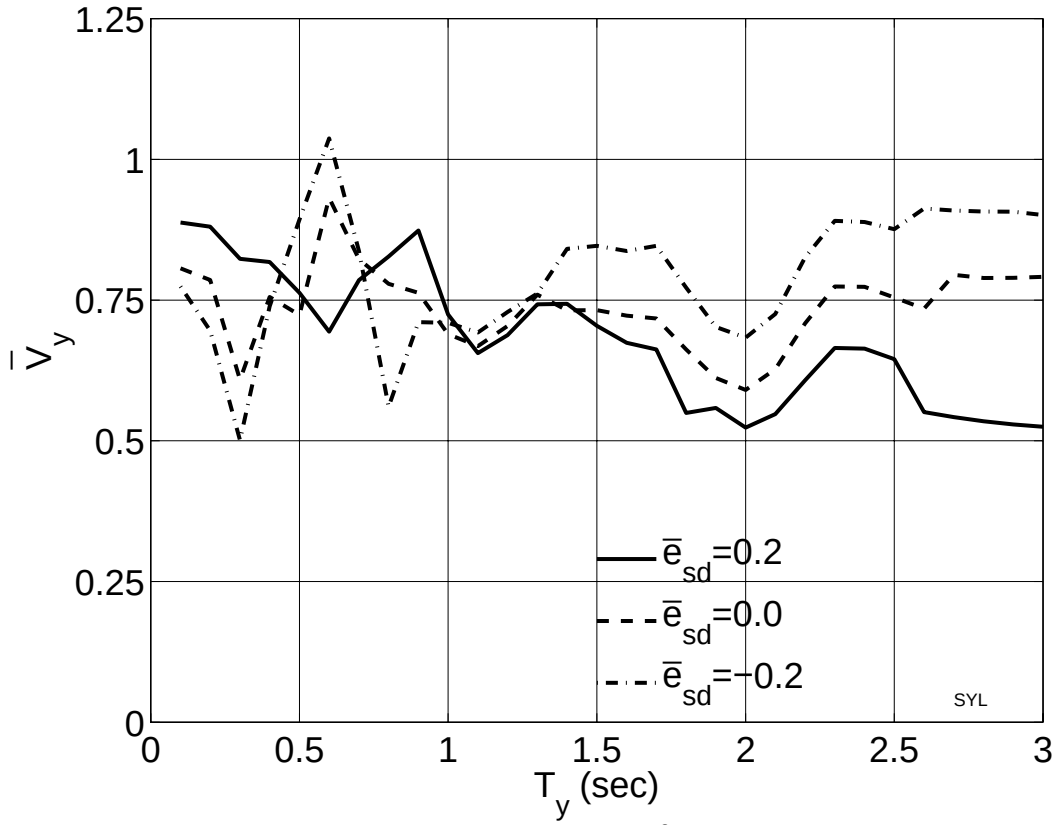

Figure 20. Normalized base shears due to elastic forces computed when total base shear is at a maximum in asymmetric-plan systems due to Sylmar earthquake ($\bar{e}_x$=0.2; $\bar{e}_y$=0; Ω_θ=1; Ω_x=1; α=2; ζ=5%) with supplemental damping (ζ_{sd}=10%; $\bar{\rho}_{sd}$=0.2)

Figure 20 shows that almost all values of $\bar{V}_b$ due to elastic forces are less than one. Values where $\bar{V}_b$ due to elastic forces are greater than one occur for $\bar{e}_{sd}$ = -0.2 for the periods between 0.6 seconds and 0.65 seconds. Figure 21 shows an upward trend for base shears due to damping forces. It can be observed that in either of the cases using $\bar{e}_{sd}$ = 0 or $\bar{e}_{sd}$ = 0.2, for the region where the period is between 1.25 seconds and 1.75 seconds, base shear due to damping forces make up an estimated 25% of the total base shear. This is also the case for $\bar{e}_{sd}$ = 0.2, for periods greater than 2.75 seconds.

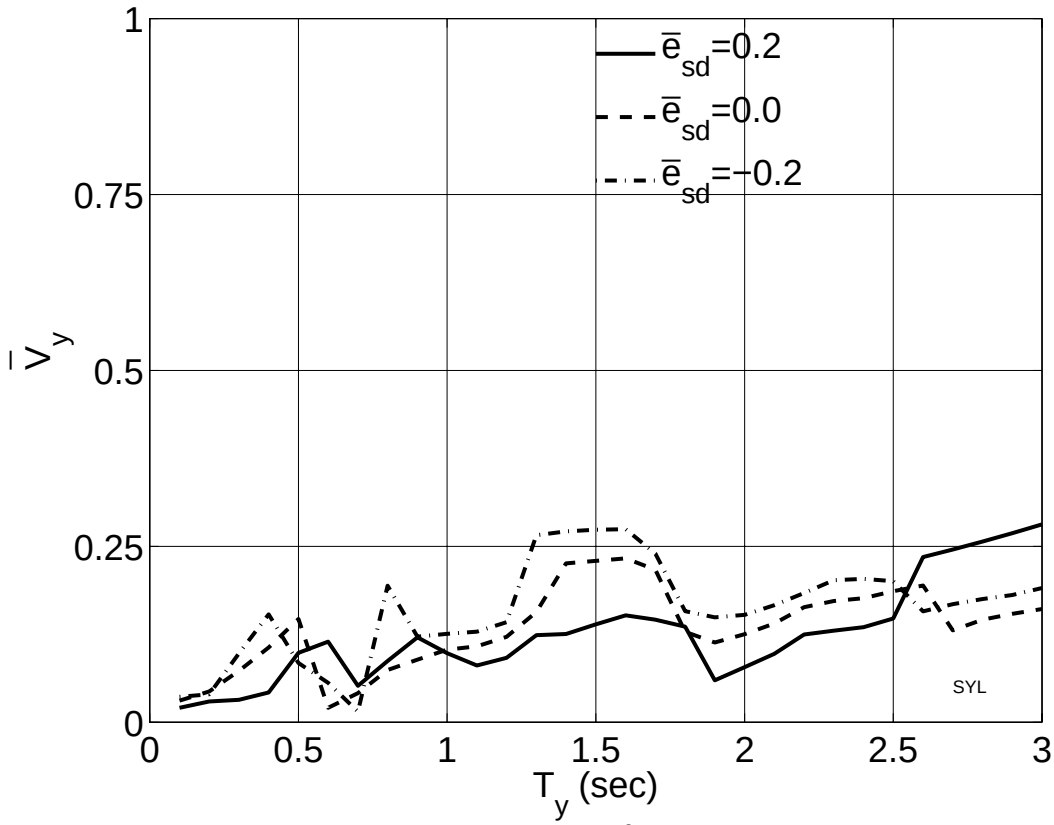

Figure 21. Normalized base shears due to damping forces computed when total base shear is at a maximum in asymmetric-plan systems due to Sylmar earthquake ($\bar{e}_x$=0.2; $\bar{e}_y$=0; Ω_θ=1; Ω_x=1; α=2; ζ=5%) with supplemental daming.

From these figures, it can be seen that the addition of damping forces contributes to higher total base shears. The results presented here so far indicate that the trends observed for the near ground motion are slightly different from the ones obtained for a broad band earthquake, such as the El Centro earthquake.

4.3 Effects of Supplemental Damping on Base Torque

The third investigation examines how plan-wise distribution of supplemental damping influences normalized base torques. The response quantity chosen is the base torque in asymmetric-plan system with supplemental damping normalized by the base torque in asymmetric-plan system without supplemental damping, $\overline{T_b} = T_{b,sd} \div T_b$. If the value of $\overline{T_b}$ is less than one, this indicates that base torque is reduced by the addition of supplemental damping as compared to base torque without supplemental damping. For a better understanding of which forces govern the total base torque, the total normalized base torque is broken down into further components, mainly the base torque due to elastic forces and the base torque due to damping forces.

Due to the El Centro earthquake, figure 22 shows the results of total normalized base torques. Values for $\overline{T_b}$ are all less than one, which indicates that supplemental damping is indeed effective in reducing base torques. As the period increases, there

seems to be an upward trend of the normalized base torques. It is hard to ascertain which supplemental damping eccentricity will lead to the largest reduction in base torque, since the trend of all three supplemental damping eccentricities fluctuate a great deal. For 0s $\leq \bar{T}_y \leq$ 0.30s, 0.55s $\leq \bar{T}_y \leq$ 0.70s, and 1.50s $\leq \bar{T}_y \leq$ 1.90s, $\bar{e}_{sd}$ = -0.2 produces the largest reduction in base torque; for periods between 2.35 and 3.00 seconds, $\bar{e}_{sd}$ = 0 produces the largest reduction in base torque; for all other periods, $\bar{e}_{sd}$ = -0.2 produces the largest reduction in base torque.

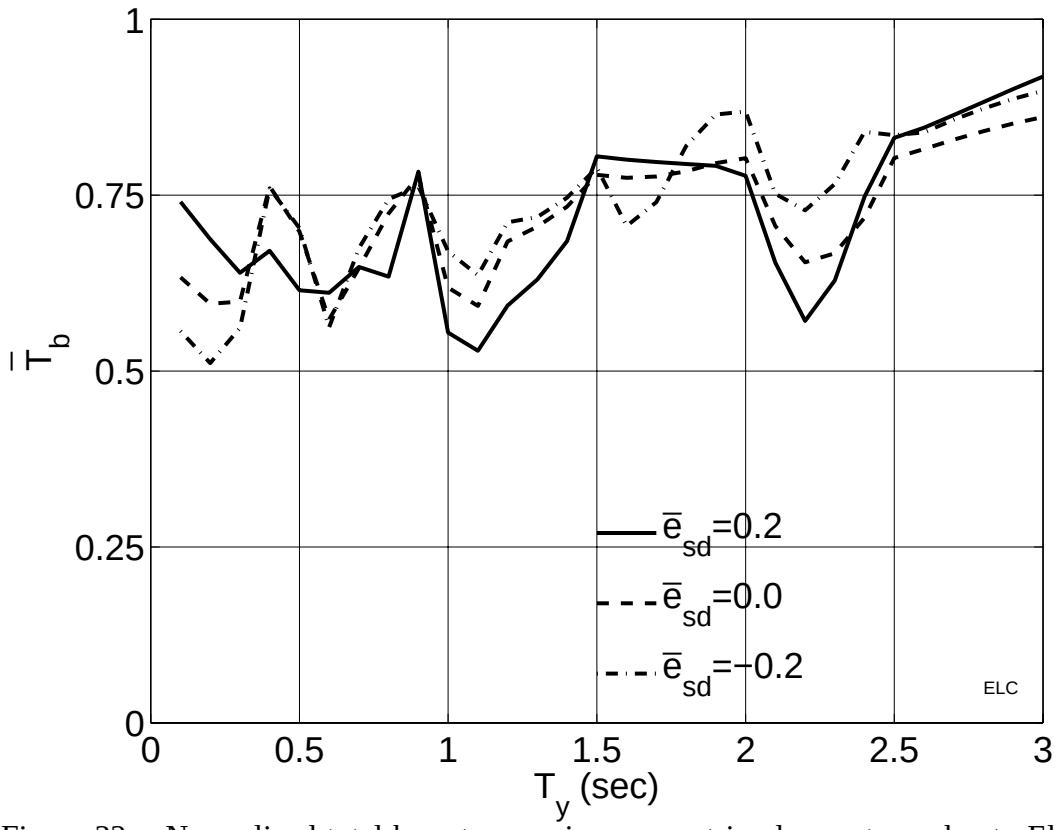

Figure 22. Normalized total base torques in asymmetric-plan systems due to El Centro earthquake ($\bar{e}_x$=0.2; $\bar{e}_y$=0; Ω_θ=1; Ω_x=1; α=2; ζ=5%) with supplemental damping (ζ_{sd}=10%; $\bar{\rho}_{sd}$=0.2)

In order to examine how much contribution of the total base torque is due to elastic forces and how much is due to damping forces, figures 23 and 24 show the results of both elastic base torques and damping base torques. Both elastic base torques and damping base torques are computed when the total base torque is at a maximum. It can be seen from these figures that base torque due to elastic forces make up approximately 75% of the total base torque, while there is very little contribution of the total base torque due to damping forces. This indicates that the elastic and damping components are

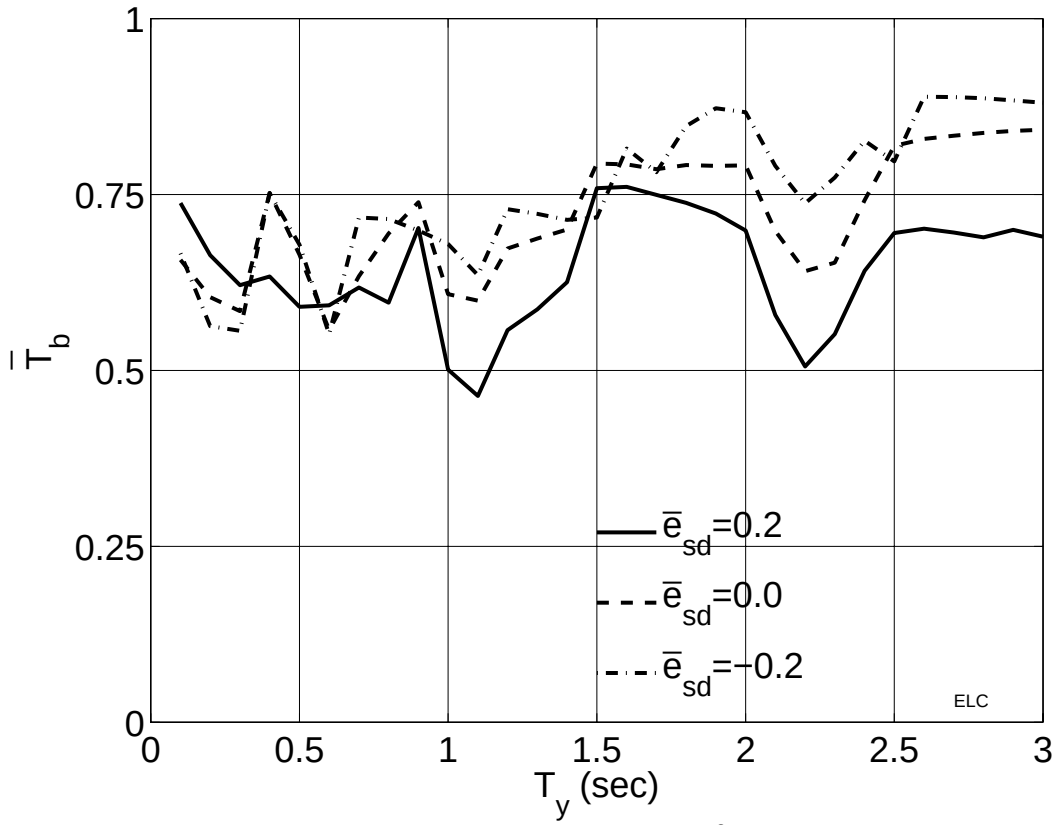

Figure 23. Normalized base torques due to elastic forces computed when total base torque is at a maximum in asymmetric-plan systems due to El Centro earthquake ($\bar{e}_x$=0.2; $\bar{e}_y$=0; Ω_θ=1; Ω_x=1; α=2; ζ=5%) with supplemental *damping* (ζ_{sd}=10%; $\bar{\rho}_{sd}$=0.2)

nearly 90° out of phase with each other. For $\bar{e}_{sd}$ = 0.2, at a period of approximately 3 seconds, it is possible to have a contribution of almost up to 25% of the total base torque due to damping forces, as can be seen from figure 24. The addition of damping forces contributes to the upward trend of total base torques, as seen in figure 22.

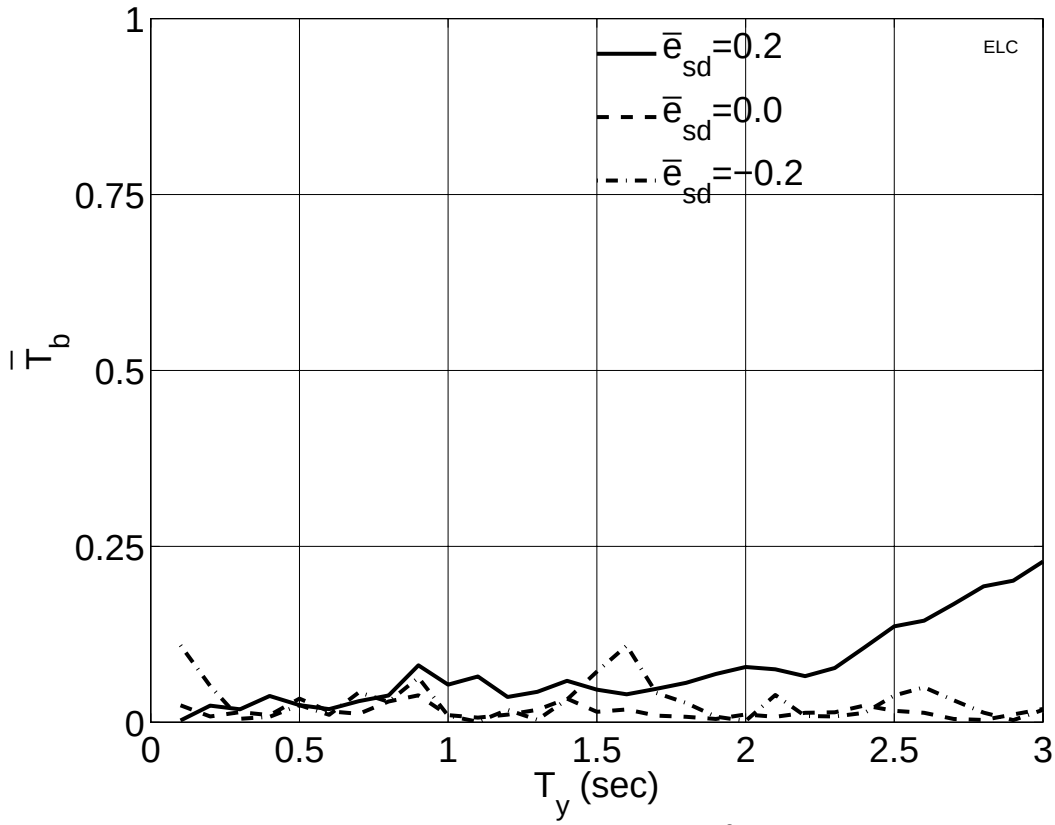

Figure 24. Normalized base torques due to damping forces computed when total base torque is at a maximum in asymmetric-plan systems due to El Centro earthquake ($\bar{e}x$=0.2; $\bar{e}y$=0; Ωθ=1; Ωx=1; α=2; ζ=5%) with supplemental damping (ζsd=10%; $\bar{\rho}sd$=0.2)

Next, to see whether or not the trends observed for the 1940 El Centro earthquake will hold for a near source earthquake, results were generated for the ground motion recorded at the Sylmar County Hospital during the 1994 Northridge earthquake. Figure 25 shows the results of total normalized base torques, due to the Sylmar earthquake. Values of $\bar{T}_b$ are all less than one, which indicates that supplemental damping is effective in reducing base torques. For periods greater than 1.4 seconds, the largest reduction of base torque can be achieved by using a supplemental damping eccentricity of 0.2. However, when it is not possible to design with $\bar{e}_{sd}$ = 0.2, it is suggested that a design for higher base torques be considered.

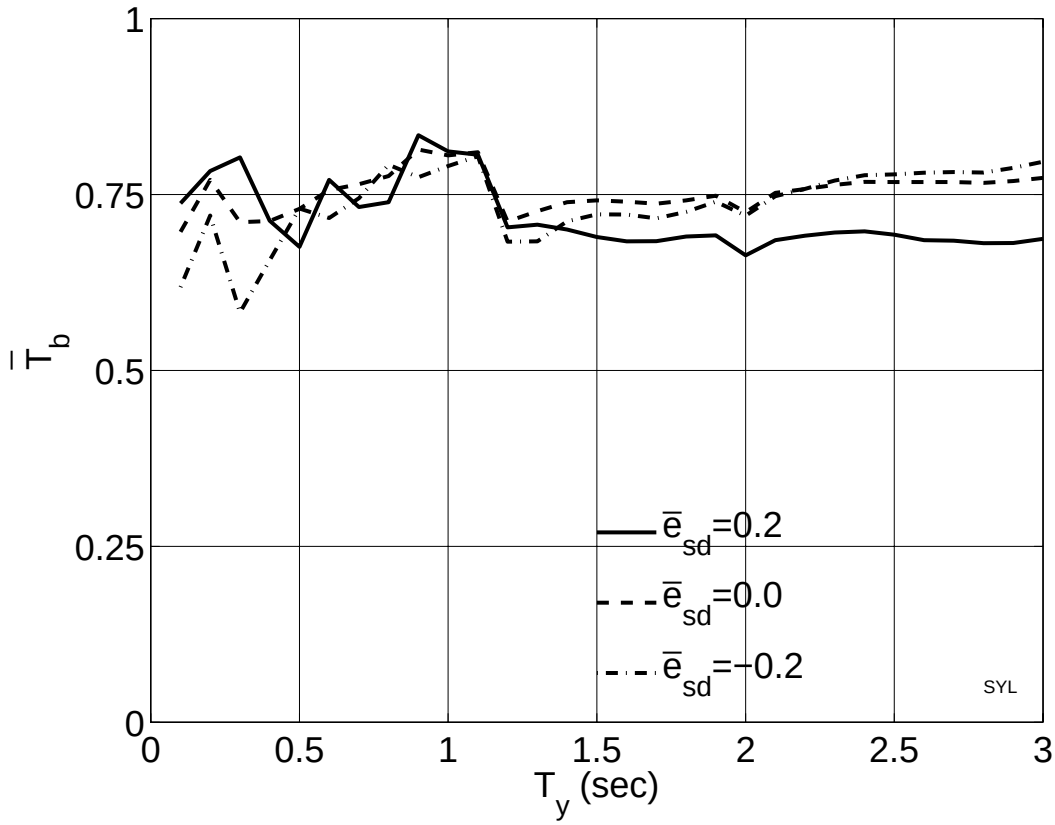

Figure 25. Normalized total base torques in asymmetric-plan systems due to Sylmar earthquake ($\bar{e}_x$=0.2; $\bar{e}_y$=0; Ω_θ=1; Ω_x=1; α=2; ζ=5%) *with supplemental damping (ζ_{sd}=10%; $\bar{\rho}_{sd}$=0.2)*

Due to the Sylmar earthquake, figures 26 and 27 depict the contributions of the total base torque due to elastic forces and damping forces. Both the elastic base torques and damping base torques are computed when the total base torque is at a maximum. It can be seen from these figures that base torque due to elastic forces make up approximately 75% of the total base torque, while there is only, perhaps, a contribution of anywhere between 5% - 10% of the total base torque due to damping forces. Trends are not as prominent for base torques. However, it can be assessed that supplemental damping does not contribute to total base torque as much as it does to total base shear.

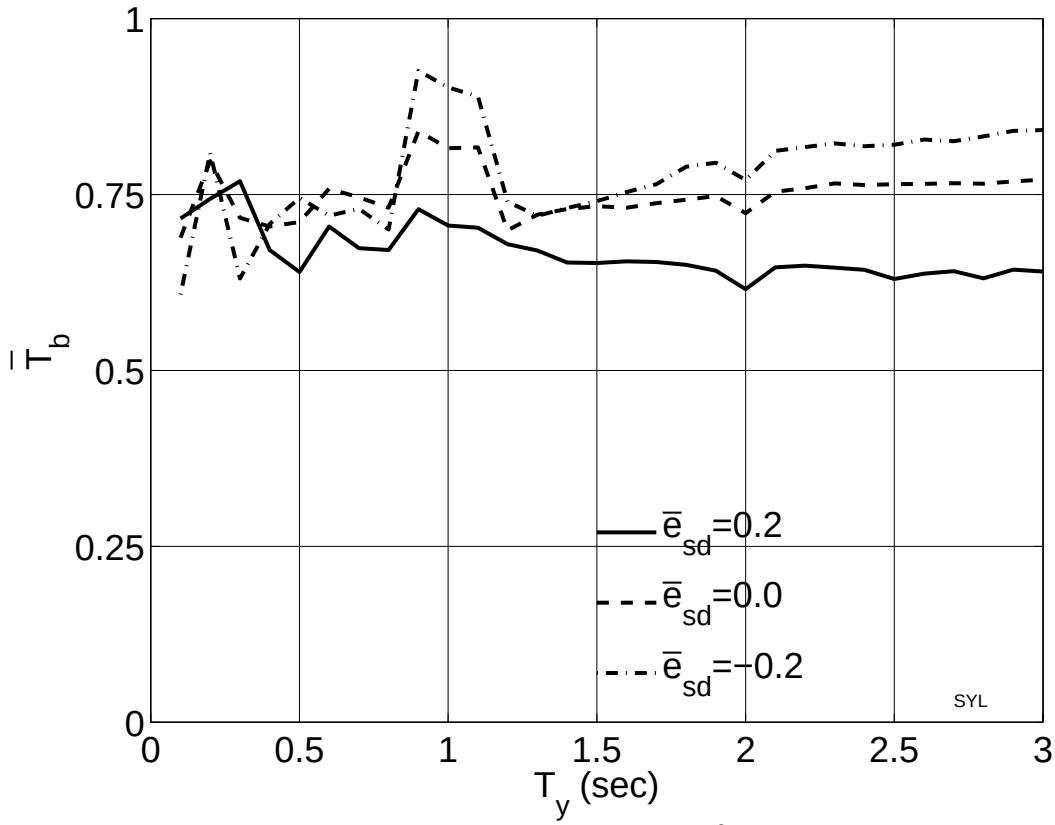

Figure 26. Normalized base torques due to elastic forces computed when total base torque is at a maximum in asymmetric-plan systems due to Sylmar earthquake ($\bar{e}_x$=0.2; $\bar{e}_y$=0; Ω_θ=1; Ω_x=1; α=2; ζ=5%) with supplemental damping (ζ_{sd}=10%; $\bar{\rho}_{sd}$=0.2).

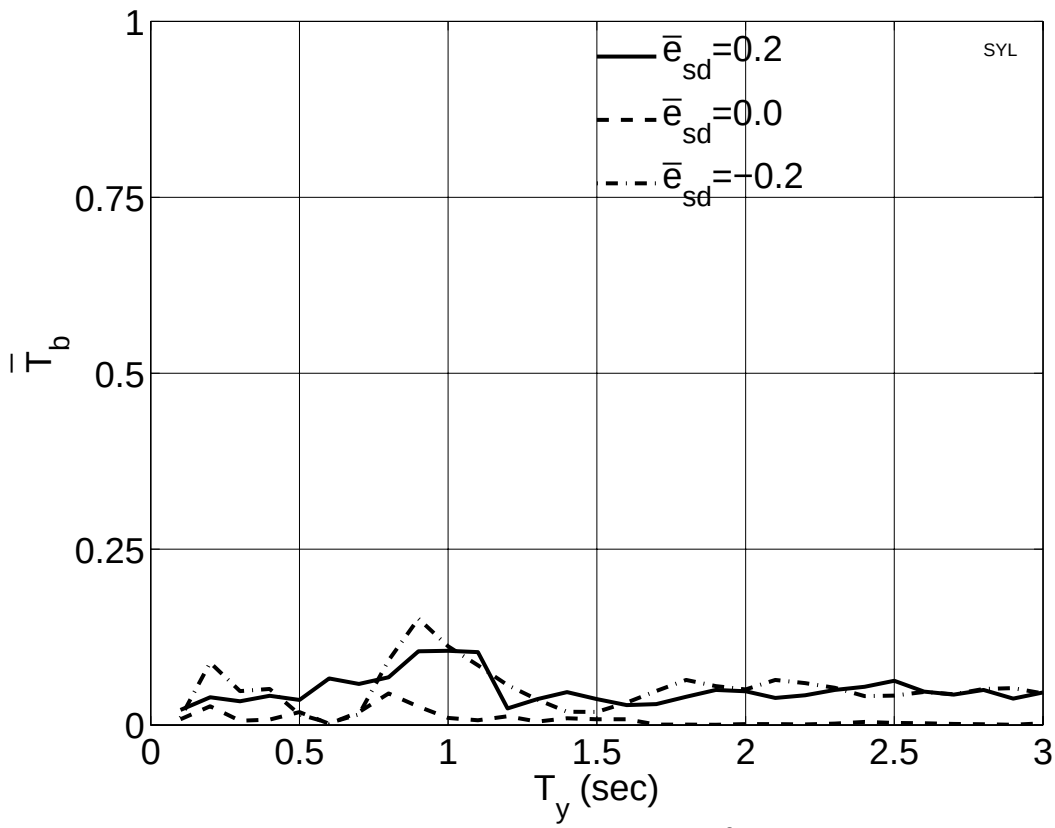

Figure 27. Normalized base torques due to damping forces computed when total base torque is at a maximum in asymmetric-plan systems due to Sylmar earthquake ($\bar{e}_x$=0.2; $\bar{e}_y$=0; Ω_θ=1; Ω_x=1; α=2; ζ=5%) with supplemental damping (ζ_{sd}=10%; $\bar{\rho}_{sd}$=0.2).

The results presented here so far indicate that the trends observed for the near ground motion are quite similar to the ones obtained for a broad band earthquake, such as the El Centro earthquake.

CHAPTER 5: CONCLUSION

After studying the effects of supplemental viscous damping on asymmetric-plan systems, it has been shown that supplemental viscous damping is indeed effective in reducing element deformations as well as base torques. In some cases, supplemental damping is also effective in reducing base shears. Elements on the flexible side as well as the stiff side are shown to have smaller displacements with supplemental damping, as opposed to without supplemental damping. In particular, the largest reduction in element deformation on the flexible side can be achieved when using a supplemental damping eccentricity of -0.2. This result suggests that all fluid viscous dampers should be placed on the flexible side, where the CSD is on the opposite side of the center of rigidity, in order to be the most effective in reducing flexible element deformations.

As for element deformations on the stiff side, the most effective results can be obtained by using a supplemental damping eccentricity of 0.2. The largest reduction in stiff element deformation is realized by placing all fluid viscous dampers on the stiff side, where the CSD is on the same side as the center of rigidity.

When examining how supplemental damping influences the trend of base shears, results indicate that in certain cases, it is possible to have higher base shears with supplemental damping than without supplemental damping. However, using a supplemental damping eccentricity of 0.2 seems to lead to the largest reduction of base shears for periods greater than 1.5 seconds. Since it is not always possible or desirable to design for such a distribution of supplemental damping, it is recommended that a design for higher base shear forces be considered.

Contributions due to both elastic forces and damping forces, which make up the total base shear, are also noted. The elastic base shears and damping base shears are computed when the total base shear is at a maximum. It is observed that both the damping forces and elastic forces are not necessarily 90° out of phase, and that the addition of damping forces contributes to higher total base shears. This occurs because earthquake loading is transient in nature and conclusions based on harmonic loading may not necessarily be applicable to this type of loading.

When examining how supplemental damping influences the trend of base torques, results show that base torques are indeed reduced by the addition of fluid viscous dampers. It is not exactly clear which supplemental damping eccentricity will produce the largest reduction of base torque, since the trend of all three supplemental damping eccentricities fluctuate a great deal. Trends for base torques are not as prominent.

Contributions due to both elastic forces and damping forces, which comprise the total base torque, are also noted. Both elastic base torques and damping base torques are computed when the total base torque is at a maximum. Again, it can be seen that both the damping forces and elastic forces are not necessarily 90° out of phase, and that the addition of damping forces contributes to higher total base torques. This occurs because earthquake loading is transient in nature and conclusions based on harmonic loading may not necessarily be applicable to this type of loading. It can be said that the base torque is most influenced by its elastic component since there is very little contribution of the total

base torque due to damping forces. Base torques due to elastic forces make up approximately 75% of the total base torque, and in some cases, it is possible to have a contribution of almost up to 25% of the total base torque due to damping forces. The results for base torques indicate that the trends observed for the near ground motion are quite similar to the ones obtained for a broad band earthquake, such as the El Centro earthquake.

It can be assessed that supplemental damping has a greater affect on total base shear than it does on total base torque. Therefore, it is vital that total base shears be carefully and properly accounted for in the process of design. This study can be used to further understand how supplemental damping affects element deformations, base shears, and base torques on asymmetric-plan systems. It is the hope of the author that these results will aid in the design of such factors as the foundation forces of structures.

BIBLIOGRAPHY

1. Constantinou, M.C. and Symans, M.D. "Seismic Response of Structures with Supplemental Damping," The Structural Design of Tall Buildings, Vol.2 (1993) : 77.

2. Hanson, Robert D. "Characteristics of Supplemental Dampers for Earthquakes," Wind and Seismic Effects, Proceedings of the 22nd Joint Meeting of the U.S.- Japan Cooperative Program in Natural Resources Panel on Wind and Seismic Effects, (Sept. 1990) : 400.

3. Goel, R.K. "Effects of Supplemental Viscous Damping on Seismic Response of Asymmetric-Plan Systems," Earthquake Engineering and Structural Dynamics, Vol.27 (1998) : 125-141.

4. Goel, R.K. "Seismic Response of Asymmetric Systems: Energy-Based Approach," Journal of Structural Engineering, (Nov. 1997) : 1444-1445.

5. Goel, R.K. "Seismic Behavior of Asymmetric Buildings with Supplemental Damping," Earthquake Engineering and Structural Dynamics, Vol.29 (2000) : 461- 481.

6. Pall, A.S. and Marsh, C. "Response of friction damped braced frames," J. Struct. Engrg., ASCE, **108**(6), (1982) : 1313-1323.

7. Pall, A.S. et al. "Friction dampers for seismic control of Concordia University Library Building," Proc. 5th Canadian Conference on Earthquake Engineering, Ottawa, Canada, (1987) : 191-200.

8. Filiatrault, A. and Cherry, S. "Performance evaluation of friction damped braced steel frames under simulated earthquake loads," Report of Earthquake Engineering Research Laboratory, University of British Columbia, Vancouver, Canada, (1985).

9. Aiken, I.D. and Kelly, J.M. "Experimental study of friction damping for steel frame structures," Proc. PVP Conference, ASME, Pittsburgh, Pennsylvania, Vol. 133 (1988) : 95-100.

10. Aiken, I.D. and Kelly, J.M. "Earthquake simulator testing and analytical studies of two-energy absorbing systems for multistory structures," Report No. UCB/EERC-90/03, University of California, Berkeley, (1990).

11. Tyler, R.G. "Tapered steel energy dissipators for earthquake resistant structures," Bulletin of the New Zealand National Society for Earthquake Engineering, **11**(4),

(1978) : 282-294.

12. Skinner, R.I. et al. "Hysteretic dampers for the protection of structures from earthquakes," Bulletin of the New Zealand National Society for Earthquake Engineering, **13**(1), (1980) : 22-36.

13. Tyler, R.G. "Further notes on a steel energy-absorbing element for braced frameworks," Bulletin of the New Zealand National Society for Earthquake Engineering, **18**(3), (1985) : 270-279.

14. Whittaker, A.S. et al. "Earthquake simulator testing of steel plate added viscoelastic dampers", Report No. UBC/EERC-89/02, University of California, Berkeley, (1989).

15. Lin, R.C. et al. "An experimental study of seismic structural response with added viscoelastic dampers", Report No. NCEER-88-0018, National Center for Earthquake Engineering Research, Buffalo, New York, (1988).

16. Chang, K.C. et al. "Seismic Response of a 2/5 scale steel structure with added viscoelastic dampers", Report No. NCEER-91-0012, National Center for Earthquake Engineering Research, Buffalo, New York, (1991).

17. Constantinou, M.C. and Symans, M.D. "Experimental Study of Seismic Response of Buildings with Supplemental Fluid Dampers," The Structural Design of Tall Buildings, Vol.2 (1993) : 93-132.

18. Foutch, D.A. et al. "Seismic Retrofit of Nonductile Reinforced Concrete Frames using viscoelastic dampers," Proceedings of a Seminar on Seismic Isolation, Passive Energy Dissipation, and Active Control, ATC-17-1, Applied Technology Council, Vol. 2 (1993) : 605-615.

19. Hanson, Robert D. "Basic Concepts and Potential Applications of Supplemental Mechanical Damping for Improved Earthquake Resistance," Proceedings of a Seminar and Workshop on Base Isolation and Passive Energy Dissipation, ATC-17, Applied Technology Council, (1986) : 39-49.

20. Hejal, R. and Chopra A.K. "Earthquake Response of Torsionally-Coupled Buildings," Report UBC/EERC-87/20, Earthquake Engineering Research Center, University of California, Berkeley, CA (1987).

21. Chopra, A.K. Dynamics of Structures: Theory and Applications to Earthquake Engineering, Prentice Hall, Upper Saddle River, NJ (1995).

22. Goel, R.K. and Booker, C. "Effects of Supplemental Viscous Damping on Inelastic Seismic Response of Asymmetric Systems," In Press, Earthquake Engineering and Structural Dynamics, (2000).

23. Kelly, J.M. et al. “Experimental testing of an energy-absorbing base isolation system,” Report No. UCB/EERC-80/35, University of California, (1980).

24. Kelly, J.M. “Base isolation in Japan, 1988,” Report No. UCB/EERC-88/20, University of California, Berkeley, (1988).

25. Goel, R.K. “Influence of Inclined Viscous Damper on Column Axial Force,” Submitted for Publication, Journal of Structural Engineering, ASCE.